6

High Performance Time-Frequency Distributions for Practical Applications

Boualem Boashash
Victor Sucic

ABSTRACT This chapter presents in three interrelated sections the key concepts and techniques needed to design and use high performance time-frequency distributions (TFDs) in real-world practical applications.

Section 6.1 first presents, in a heuristic approach, the *core concepts* forming the field of time-frequency signal processing, incorporating recent developments, such as the design of high resolution quadratic TFDs for multicomponent signal analysis.

Section 6.2 outlines *methods of assessment* of the performance of time-frequency techniques, in terms of the resolution performance of TFDs in separating closely spaced components in the time-frequency domain. A performance measure is defined using key attributes of TFDs, such as the components' mainlobes and sidelobes, and cross-terms. This method of assessment of TFDs performance has led to improvements in designing high resolution quadratic TFD for time-frequency analysis of multicomponent signals.

Section 6.3 presents a *methodology* for selecting the optimal TFD for a given real-life signal under application-specific constraints. The methodology, based on the performance measure, allows for emphasis of signal features in specific regions of interest in the time-frequency domain.

6.1 The core concepts of time-frequency signal processing

6.1.1 Rationale for using time-frequency distributions

In order to provide more insight into the nature of nonstationary signals, a new field of science and engineering has emerged: the field of joint time-frequency signal processing (TFSP).

The introduction of TFSP has led to new tools to represent and characterize the time-varying contents of nonstationary signals using time-frequency distributions (TFDs), the most popular ones belonging to the class of quadratic distributions (see

Eq. (6.1.20)). By distributing the signal energy over the time-frequency plane, TFDs provide the analyst with information unavailable from the signal time-domain representation or its frequency-domain representation. This includes the number of components present in the signal, the time durations and frequency bands over which these components are defined, the components' relative amplitudes, phase information, and the instantaneous frequency (IF) laws that components follow in the time-frequency plane.

The essential characteristic of TFSP is that it comprises a set of signal processing methods, techniques, and algorithms in which the two natural variables time, t, and frequency, f, are used *concurrently*. This contrasts with the traditional signal processing methods in which time and frequency variables are used *exclusively* and *independently*. Nature shows us in our daily experiences that the two variables, t and f, are usually simultaneously present in signals (e.g., the speech of a person, the song of a bird, or music played on the radio). Such signals are called "nonstationary" signals because their spectral characteristics vary with time. This chapter considers signals that have finite duration T and nearly finite bandwidth B; these signals are often referred to as asymptotic, with the degree of asymptoticity expressed by the BT product [3]. TFSP is designed to deal effectively with such signals by allowing a more detailed analysis and processing.

In addition to existing methods of TFSP, special-purpose TFDs could be defined to suit the particular class of signals under investigation. This chapter presents a simple approach for TFD design. For this purpose, we first revisit the core concepts of TFSP from a practical point of view (Section 6.1), and investigate the performance criteria for TFDs from a user's point of view. The performance of TFDs [1,2] is assessed in terms of *concentration* and *resolution*, and an optimization procedure is used to select the optimal parameter values of TFDs (Section 6.2). Finally, we define a methodology for selecting the most suitable TFD in a given practical situation (Section 6.3).

6.1.2 *Limitations of traditional signal representations*

The spectrum of a signal (deterministic or random) gives no indication as to how the frequency content of a signal changes with time—information that is important when one deals with frequency modulated (FM) signals or other kinds of nonstationary signals. This frequency variation often contains crucial information about the signal and process studied in applications.

The limitation of "classical" spectral representations is better illustrated by the fact that we can find totally different signals (related to different physical phenomena), $s_a(t)$ and $s_b(t)$, which yet have the same "spectra" (that is, magnitude spectra). The following example shows the inherent limitation of conventional spectral analysis.

Example 6.1. Consider the two signals, $s_a(t)$ (finite duration linear FM) and $s_b(t)$ (infinite duration sinc function), defined as

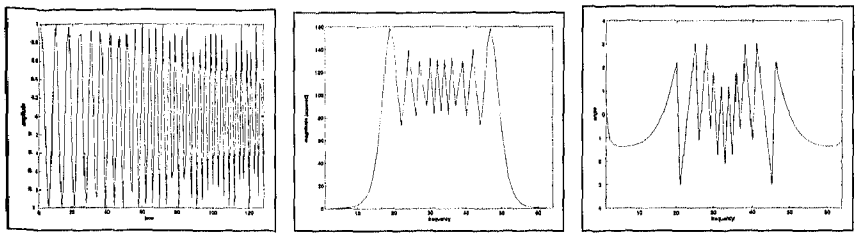

(a) Time domain (b) Magnitude spectrum (c) Phase spectrum

FIGURE 6.1. Time-domain and frequency-domain representations of the finite duration linear FM signal $s_a(t)$ defined by Eq. (6.1.1).

$$s_a(t) = \begin{cases} \cos\left[2\pi\left(f_0 t + \alpha\frac{t^2}{2}\right)\right], & 0 < t < T \\ 0, & \text{elsewhere} \end{cases} \tag{6.1.1}$$

$$s_b(t) = \frac{\sin(\pi B t)}{\pi t}\cos(2\pi f_c t), \tag{6.1.2}$$

where f_0 is the start frequency, $\alpha = B/T$ represents the rate of the frequency change, and $f_c = f_0 + B/2$.

The signal $s_a(t)$ is nonstationary: it is a linear FM signal commonly used in radar and seismic applications (it is analogous to a musical note with a steadily rising pitch). Equation (6.1.1) indicates that the signal $s_a(t)$ is a cosine function in the interval $(0, T)$, and zero outside this interval. Figures 6.1 and 6.2 show the time representation and the frequency representation of the signals $s_a(t)$ and $s_b(t)$, respectively.

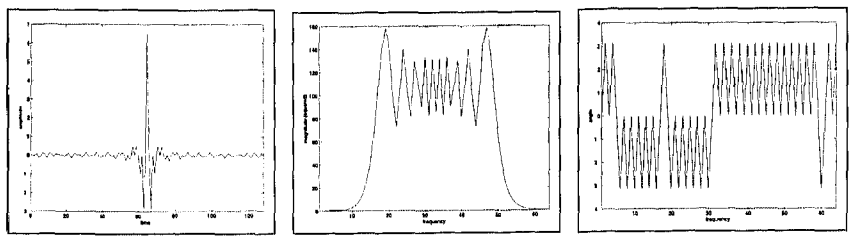

(a) Time domain (b) Magnitude spectrum (c) Phase spectrum

FIGURE 6.2. Time-domain and frequency-domain representations of the infinite duration sinc signal $s_b(t)$ defined by Eq. (6.1.2).

Although the signals $s_a(t)$ and $s_b(t)$ are fundamentally different, they have the same magnitude squared spectrum (Figures 6.1(b) and 6.2(b)). The information that allows one to discriminate between them is contained in their phase spectra (Figures 6.1(c) and 6.2(c)), which is lost when we form the square modulus of the Fourier transform (FT). The frequency in the signal $s_a(t)$ is steadily rising with time, a fact not revealed by the signal spectrum displayed in Figure 6.1(b), which only shows a constant amplitude broadband spectrum.

It follows then that the magnitude spectrum by itself is insufficient (and hence inadequate) for representing signals in a way useful for precise characterization and identification. This serves as a part of the motivation for devising a more "sophisticated" and "practical" nonstationary signal analysis tool, which preserves "all" the information of the signal and discriminates signals in a better way, using a single complete representation instead of attempting to interpret signals' magnitude and phase spectra separately.

6.1.3 *Positive frequencies and the analytic signal*

An important property of the FT is that for $s(t)$ real, its FT, $S(f)$, is complex and has Hermitian symmetry ($S(f) = S^*(-f)$); i.e., its real part and magnitude are even symmetric, and its imaginary part and phase are odd symmetric. The information contained in the negative frequencies is therefore a duplication of the information contained in the positive frequencies. As a frequency represents the number of oscillations of a signal observed in a second, a frequency is expected to be positive. The negative frequencies appear in the spectrum of a real signal as a consequence of the mathematical model of the FT. In practice, a signal analyst would prefer to deal only with positive frequencies. This is achieved by introducing a complex signal called the analytic signal.

Definition 6.1. An analytic signal $z(t)$ is a complex signal that contains only positive frequencies, such that its FT, $Z(f)$, satisfies

$$Z(f) = 0, \qquad \text{for } f < 0. \tag{6.1.3}$$

A real signal $x(t)$ cannot have only positive frequencies, as the FT of $x(t)$ has a Hermitian symmetry, which contradicts the hypothesis of $X(f) = 0$ for $f < 0$.

Theorem 6.1. *A complex signal $z(t) = x(t) + j\,y(t)$ is analytic if and only if its real and imaginary parts are related as follows:*

$$y(t) = x(t) \star \frac{1}{\pi t} \equiv \mathcal{H}\{x(t)\}, \tag{6.1.4}$$

where $\star$ denotes the convolution in time t and $\mathcal{H}\{\cdot\}$ is the Hilbert transform:

$$\mathcal{H}\{x(t)\} = p.v. \left\{ \int_{-\infty}^{\infty} \frac{x(t-\tau)}{\pi\tau}\, d\tau \right\} \tag{6.1.5}$$

with p.v. being the principal value of Cauchy's integral.

Theorem 6.2. *If $s(t)$ is a real signal expressed as $s(t) = a(t)\cos\phi(t)$, then under the conditions outlined in [4], and using the fact that $\mathcal{H}\{a(t)\cos\phi(t)\} = a(t)\,\mathcal{H}\{\cos\phi(t)\}$, we can construct an analytic signal $z(t)$ which corresponds to $s(t)$ by replacing $\cos\phi(t)$ by $e^{j\phi(t)}$; that is, $z(t) = a(t)\,e^{j\phi(t)}$ and $s(t)$ is the real part of $z(t)$.*

This theorem is important for practical applications because it shows a relation of equivalence between the real signal $s(t)$ and its analytic associate $z(t)$.

6.1.4 *Joint time-frequency representations*

6.1.4.1 Uncovering hidden information using time-frequency representations

Revealing the time and frequency dependence of a signal, such as the signal $s_a(t)$ in Example 6.1, is achieved by using a joint time-frequency representation. In Figure 6.3, the Wigner–Ville distribution (Eq. (6.1.16)) is used to represent $s_a(t)$, as it provides the optimal joint time-frequency representation for a chirp (linear FM) signal [3].

In Figure 6.3, the signal start and stop times are clearly identifiable from its time-frequency representation, as is the time variation of the frequency content of the

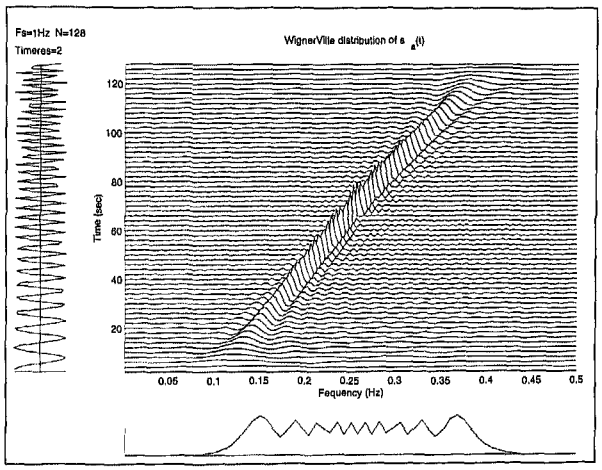

FIGURE 6.3. Time-frequency representation (Wigner–Ville distribution) of the linear FM signal $s_a(t)$ defined by Eq. (6.1.1). The signal's time domain representation is given on the left, and its magnitude spectrum on the bottom.

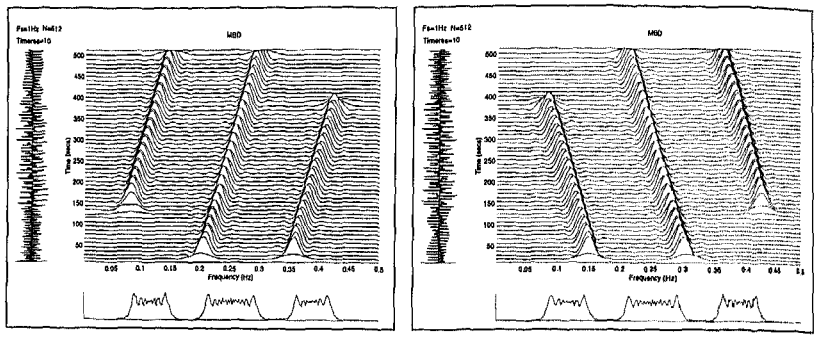

(a) Modified B distribution of the first signal

(b) Modified B distribution of the second signal

FIGURE 6.4. Time-frequency representation (Modified B distribution) of two different three-component signals.

signal. This information cannot be retrieved solely from either the signal instantaneous power $|s(t)|^2$ or its spectrum $|S(f)|^2$ representation. The ease of interpreting plots such as the plot in Figure 6.3 makes the concept of a joint time-frequency signal representation attractive.

Example 6.2. Figure 6.4 illustrates another case of two different signals having similar magnitude spectra. Both signals contain three linear FM components. The differences in the time intervals, frequency bands, and the FM laws that characterise the signals' components are not shown clearly in the t domain and the f domain, but do appear clearly in the signals' (t, f) representation (here the Modified B distribution (MBD) [5]).

Example 6.2 shows that another advantage of using a joint time-frequency representation of signals is that it reveals whether the signal is monocomponent or multicomponent [3, 6], a fact that cannot be easily obtained from the signal time-domain or frequency-domain representation.

6.1.4.2 What is a time-frequency representation?

TFSP is a "natural" extension of both time-domain and frequency-domain processing, that involves representing signals in a complete space that can display "all" the signal information in a more accessible way [6]. Such a representation is intended to provide a *distribution* of signal energy versus both time and frequency simultaneously. For this reason, the representation is commonly called a TFD, and is denoted $\rho_z(t, f)$.

A concept intimately related to joint time-frequency representation is that of IF and time delay. The IF corresponds to the frequency of a sine wave that locally (at a

given time) fits the signal under analysis. The time delay is a measure of the "order of arrival" of the frequencies.

The TFD is expected to visually exhibit in the (t, f) domain the time-frequency law of each signal component, thereby making the estimation of their IFs and time delays easier, and should also provide additional information about components' relative amplitudes, and the spectral spread of the components around their IFs (the spread is known as the instantaneous bandwidth [3, 6, 7]). For example, the ridges in Figure 6.4 indicate that the three signal components have equal amplitudes, and the peaks of these ridges reveal the linear FM laws of the components. All components have the same instantaneous bandwidth around their IFs, as indicated by the same concentration the ridges attain about their peaks.

6.1.4.2.1 Instantaneous frequency and time delay

The instantaneous frequency of a monocomponent signal is a measure of the localization in time of the individual frequency components of the signal [4].

The IF, $f_i(t)$, of a monocomponent *analytic* signal $z(t) = a(t)e^{j\phi(t)}$ is given by

$$f_i(t) = \frac{1}{2\pi}\frac{d\phi(t)}{dt}. \tag{6.1.6}$$

The IF of a monocomponent *real* signal $s(t) = a(t)\cos\phi(t)$ is defined as the IF of the analytic signal $z(t)$ corresponding to $s(t)$.

The dual of the IF concept in the frequency domain is called the "time delay." The time delay, $\tau_d(f)$, of a monocomponent *analytic* signal $z(t)$ is defined as

$$\tau_d(f) = -\frac{1}{2\pi}\frac{d\theta(f)}{df}, \tag{6.1.7}$$

where

$$\mathcal{F}\{z(t)\} = Z(f) = A(f)e^{j\theta(f)} \tag{6.1.8}$$

is the FT of $z(t)$.

The time delay of a monocomponent *real* signal $s(t)$ is defined as the time delay of the analytic signal $z(t)$ corresponding to $s(t)$.

The order of appearance of each time-varying frequency component is the time delay. The global order of appearance of the frequencies is called the *group delay* (a mean value of individual time delays). The group delay equivalent for IFs is the *mean* IF.

The IF and the time delay describe the "internal organization" of the signal. The use of time-domain representations *or* frequency-domain representations leads one to effectively neglect this information, resulting in a scrambling of the information contained in the signal, as illustrated in Examples 6.1 and 6.2.

6.1.4.2.2 *Physical interpretation of TFDs*

Most TFDs used for a practical time-frequency signal analysis are not necessarily positive, so they do not represent an instantaneous energy spectral density at time t and frequency f. For example, the Page distribution is defined as the time derivative of the "running spectrum" (spectrum of the signal from $-\infty$ to time t), and hence can take both positive and negative values [8]:

$$\rho_z(t,f) = \frac{\partial}{\partial t}\left|\int_{-\infty}^{t} z(u)e^{-j2\pi fu}du\right|^2.$$

To relate $\rho_z(t,f)$ to the physical quantities used in practical experimentation, we interpret $\rho_z(t,f)$ as a measure of energy flow through the spectral window $(f-\Delta f/2, f+\Delta f/2)$ during the time interval $(t-\Delta t/2, t+\Delta t/2)$. The signal energy localized in the time-frequency region $(\Delta t, \Delta f)$ is then given by [3]

$$E_{\Delta t,\Delta f} = \int_{t-\Delta t/2}^{t+\Delta t/2}\int_{f-\Delta f/2}^{f+\Delta f/2} \rho_z(t,f)\, df\, dt. \tag{6.1.9}$$

The spectral window should be chosen large enough so that the product $\Delta t \Delta f$ satisfies the Heisenberg uncertainty relation [9]:

$$\Delta t\, \Delta f \geq 1/(4\pi). \tag{6.1.10}$$

With this interpretation, negative values of $\rho_z(t,f)$ are then accounted for, and positivity can be removed as a requirement. This is especially important since positivity is also incompatible with the requirement that the signal IF is the first moment of its TFD with respect to frequency [3].

6.1.4.2.3 *Desirable properties and criteria for a TFD*

The TFD is expected to satisfy a certain number of properties that are intuitively desirable for a practical analysis. It was reported in [3] that a TFD should satisfy the marginals; i.e., a TFD should reduce to the spectrum and instantaneous power by integrating over t, respectively f. Furthermore, a TFD is expected to have the IF as its first moment with respect to frequency. These strict constraints on the TFD design led to the terminology of Cohen's class [10].

However, our approach is different and more in line with actual *usage and practice*. We first note that many popular TFDs (e.g., the spectrogram) do not satisfy the marginals and the IF moment condition. Yet the spectrogram has been a valuable tool in many practical applications, suggesting that the time and the frequency marginal and the IF moment constraints may not be strictly needed in practice. What is more important in most practical applications is to maximize the energy concentration about the IF for monocomponent signals and improve the resolution for multicomponent signals.

We have found from practical experience that a time-frequency representation of signal $z(t)$, $\rho_z(t,f)$, needs to satisfy the following properties, so that it can be useful

for practical purposes and not just for theoretical interest [2, Part I].

• P1 (*Reality and energy*): The TFD should be real, and its integration over the whole time-frequency domain should be equal to the energy of the signal $z(t)$, E_z:

$$\int_{-\infty}^{\infty}\int_{-\infty}^{\infty} \rho_z(t,f)\,dt\,df \equiv E_z. \tag{6.1.11}$$

• P2 (*Distribution of energy*): The signal energy in a certain region R in the (t,f) plane, E_{z_R}, should be obtained by integrating $\rho_z(t,f)$ over the boundaries $(\Delta t, \Delta f)$ of the region R:

$$\int_{\Delta t}\int_{\Delta f} \rho_z(t,f)\,df\,dt = E_{z_R}. \tag{6.1.12}$$

E_{z_R} is a portion of signal energy in the frequency band Δf and time interval Δt. Note that Δf and Δt need to be selected in such a way that the uncertainty principle (Eq. (6.1.10)) is satisfied. Property P2 is equivalent to Eq. (6.1.9).

• P3 (*IF peak property*): The peak of the time-frequency representation of a monocomponent FM signal with respect to frequency should reflect the IF of the signal:

$$\left.\frac{\partial \rho_z(t,f)}{\partial f}\right|_{f=f_i(t)} = 0. \tag{6.1.13}$$

For multicomponent signals, the same property should apply to the individual components.

• P4 (*Concentration and resolution*): The TFD of a monocomponent FM signal is expected to have a good energy *concentration* around the signal IF law. For a multicomponent FM signal, a TFD is expected to provide a good (t,f) *resolution* of the signal components. This requires a good energy concentration for each of the components and the suppression of any undesirable artifacts.

• P5 (*Robustness to noise*): When a signal embedded in additive white noise is analyzed in the joint time-frequency plane, the noise becomes evenly spread in the plane [3]. For moderate to high signal-to-noise ratios, the signal components dominate over noise in the time-frequency domain, so their IF laws can be estimated from the TFD's dominant peaks (Property P3), provided the TFD satisfies Property P4. It is desirable that such obtained IF estimates are as close as possible to the signal components' true IF laws, i.e., that they are minimum bias and minimum variance IF estimates.

Naturally, the following questions arise: Is there a TFD that meets specifications P1–P5? If yes, how do we construct it? What are the significant signal characteristics and parameters that impact on the design of such a TFD? How do these relate to the TFD itself? How do we obtain them from the actual designed TFD? These questions are answered in the following sections of this chapter.

6.1.5 *Heuristic formulation of the class of quadratic TFDs*

6.1.5.1 Time-varying spectrum and the Wigner–Ville distribution

Considering the basic definition of the power spectrum density (PSD), let us determine why time information seems to disappear when we take the PSD, and how it can be restored.

Let us consider a complex random process $Z(t)$ with realizations $z(t,\epsilon)$, where ϵ represents the ensemble index identifying each realization. Using context, rather than explicit rigorous mathematical formulation, to improve clarity we simply replace $z(t,\epsilon)$ by $z(t)$. Thus, ϵ is implicit when we say that $z(t)$ is random.

The Wiener–Khintchine theorem states that for a stationary signal, the signal PSD equals the FT of its autocorrelation function [11]. By extension to nonstationary random signals, the time-varying PSD, $S_z(t,f)$, is then defined as the FT of the time-varying autocorrelation function, $R_z(t,\tau)$.

The time-varying autocorrelation function of $z(t)$ is defined in symmetric form as [3]

$$\begin{aligned} R_z(t,\tau) &= \mathcal{E}\{z(t+\tau/2)z^*(t-\tau/2)\} \\ &= \mathcal{E}\{K_z(t,\tau)\}, \end{aligned} \tag{6.1.14}$$

where $K_z(t,\tau) = z(t+\tau/2)z^*(t-\tau/2)$ is the *signal kernel* and $\mathcal{E}\{\cdot\}$ defines the expected value operator.

Therefore, the signal time-varying PSD $S_z(t,f)$ is given as

$$\begin{aligned} S_z(t,f) &= \underset{\tau\to f}{\mathcal{F}} \{R_z(t,\tau)\} \\ &= \underset{\tau\to f}{\mathcal{F}} \{\mathcal{E}\{K_z(t,\tau)\}\} \\ &= \mathcal{E}\left\{\underset{\tau\to f}{\mathcal{F}} \{K_z(t,\tau)\}\right\} \\ &= \mathcal{E}\{W_z(t,f)\}, \end{aligned} \tag{6.1.15}$$

where the interchange of $\mathcal{E}\{\cdot\}$ and FT is made under assumptions verified by most practical signals and asymptotic signals [3]; and $W_z(t,f)$ denotes the Wigner–Ville distribution (WVD) of $z(t)$, expressed as

$$\begin{aligned} W_z(t,f) &= \underset{\tau\to f}{\mathcal{F}}\{K_z(t,\tau)\} \\ &= \underset{\tau\to f}{\mathcal{F}}\{z(t+\tau/2)z^*(t-\tau/2)\} \\ &= \int_{-\infty}^{\infty} z(t+\tau/2)z^*(t-\tau/2)\, e^{-j2\pi f\tau}\, d\tau. \end{aligned} \tag{6.1.16}$$

The problem of estimating the time-varying PSD of a random process $z(t)$ thus reduces to averaging the WVD of the process over ϵ. If only one realization of the process is available, assuming the process is locally ergodic [11] over a time window, an estimate of the process time-varying PSD is obtained by smoothing the WVD over the window of local ergodicity [3].

6.1.5.2 Time-varying spectrum estimates and quadratic TFDs

If $z(t)$ is deterministic, from Eq. (6.1.15), $S_z(t,f)$ reduces to $W_z(t,f)$:

$$S_z(t,f) = \mathcal{E}\{W_z(t,f)\} = W_z(t,f). \tag{6.1.17}$$

The signals we consider in this chapter are asymptotic (most real-life signals), having a finite duration T, and a finite bandwidth B [3]. The finite duration of a signal is obtained by windowing the signal with a finite duration time function $g(t)$, hence convolving $S_z(t,f)$ in the frequency domain with $G(f) = \underset{t\to f}{\mathcal{F}}\{g(t)\}$.

The finite bandwidth restriction is met by windowing the signal in the frequency domain with a band-limited function $H(f)$, hence convolving $S_z(t,f)$ in the time domain with $h(t) = \underset{f\to t}{\mathcal{F}}^{-1}\{H(f)\}$.

By combining the separate windowing effects of $g(t)$ in time and $H(f)$ in frequency, the estimate of the signal time-varying PSD can be defined as

$$\hat{S}_z(t,f) = G(f) \star_f W_z(t,f) \star_t h(t), \tag{6.1.18}$$

where $G(f)$ and $h(t)$ are even functions (such as those traditionally used in spectral analysis and digital filter design), and $\star_t$ and $\star_f$, respectively, denote the convolution in time and convolution in frequency.

The preceding formulation for $\hat{S}_z(t,f)$ was introduced step by step to illustrate the two-dimensional (2D) convolution that is inherent to most real-life signals. This formulation, however, corresponds to a special case where the 2D windowing in t and f is separable.

In the general case, we need to introduce an even function $\gamma(t,f)$, which may or may not be separable, that reflects the signal overall duration-bandwidth limitations in both time and frequency. This leads to the following general formulation of time-frequency representations $\rho_z(t,f)$ of signal $z(t)$ [2, Part I]:

$$\hat{S}_z(t,f) \equiv \rho_z(t,f) = W_z(t,f) \star_t \star_f \gamma(t,f), \tag{6.1.19}$$

where $\gamma(t,f)$ is an even function that defines the TFD $\rho_z(t,f)$ and its properties, and $\star_t\star_f$ denotes the convolution in both time and frequency.

By expanding $W_z(t,f)$ and the double convolution in Eq. (6.1.19), we obtain the following *general quadratic form* of TFDs [2, Part I]:

$$\rho_z(t,f) = \int_{-\infty}^{\infty}\int_{-\infty}^{\infty}\int_{-\infty}^{\infty} e^{j2\pi\nu(u-t)} g(\tau,\nu) z\Big(u+\frac{\tau}{2}\Big) z^*\Big(u-\frac{\tau}{2}\Big) e^{-j2\pi f\tau}\, d\nu\, du\, d\tau, \tag{6.1.20}$$

where $g(\tau,\nu)$, known as the TFD *kernel filter*, is the 2D FT of $\gamma(t,f)$.

The function $g(\tau,\nu)$ is analogous to the windows used in classical spectral analysis, and it determines how the signal energy is distributed in time and frequency.

By appropriately choosing $g(\tau, \nu)$ in Eq. (6.1.20), we can obtain most of the popular time-frequency representations of $z(t)$, such as those defined in [2, Part I].

Eq. (6.1.20) differs from Cohen's class [7,10] by the sign in the first exponential. This allows for fewer restrictions on the choice of kernel filter, as discussed in Subsection 6.2.3, and the interpretation of $\rho_z(t, f)$ as a filtered version of the WVD, as explained in Subsection 6.1.5.3.

6.1.5.3 Time, lag, frequency, Doppler domains, and the ambiguity function

We have defined in Eq. (6.1.16) the WVD of signal $z(t)$ as the FT of the signal kernel $K_z(t, \tau)$:

$$W_z(t, f) = \underset{\tau \to f}{\mathcal{F}}\{K_z(t, \tau)\}. \tag{6.1.21}$$

The representation $W_z(t, f)$ is a function of two variables, t and f.

The time-averaged autocorrelation function of signal $z(t)$ may be defined as

$$R_z(\tau) = \int_{-\infty}^{\infty} z(t + \frac{\tau}{2}) z^*(t - \frac{\tau}{2})\, dt. \tag{6.1.22}$$

$R_z(\tau)$ describes the similarity between the signal and its time-delayed copies. It is obtained by taking the integral over time of the signal kernel $K_z(t, \tau)$.

Another quantity that relates to $K_z(t, \tau)$ is the symmetric ambiguity function [2,3]:

$$\begin{aligned} A_z(\tau, \nu) &= \int_{-\infty}^{\infty} K_z(t, \tau)\, e^{-j2\pi\nu t} dt \\ &= \int_{-\infty}^{\infty} z(t + \frac{\tau}{2}) z^*(t - \frac{\tau}{2})\, e^{-j2\pi\nu t} dt. \end{aligned} \tag{6.1.23}$$

Equation (6.1.23) represents the basic radar equation obtained by correlating a signal with the same signal delayed in time by lag τ and shifted in frequency by Doppler ν.

Thus, $K_z(t, \tau)$ is the key element in the formulation of many important TFSP concepts. Time-frequency (t, f), time-lag (t, τ), lag-Doppler (τ, ν), and Doppler-frequency (ν, f) representations can be obtained from the signal kernel $K_z(t, \tau)$ by means of the FT and the inverse FT [2, Part I]. This is illustrated in Figure 6.5.

As shown in Figure 6.5, the 2D FT (indicated by two vertical arrows) of the WVD of signal $z(t)$ equals the symmetric ambiguity function $A_z(\tau, \nu)$ of $z(t)$ [2, Part I]:

$$W_z(t, f) \overset{t}{\underset{f}{\rightleftharpoons}} \overset{\nu}{\underset{\tau}{}} A_z(\tau, \nu). \tag{6.1.24}$$

This is an important relationship in TFSP because it indicates that the dual of the time-frequency domain is the lag-Doppler domain (also called the ambiguity domain). The (t, f) domain represents the signal as a function of actual time and actual frequency, and the (τ, ν) domain represents the signal as a function of time shifts and frequency shifts.

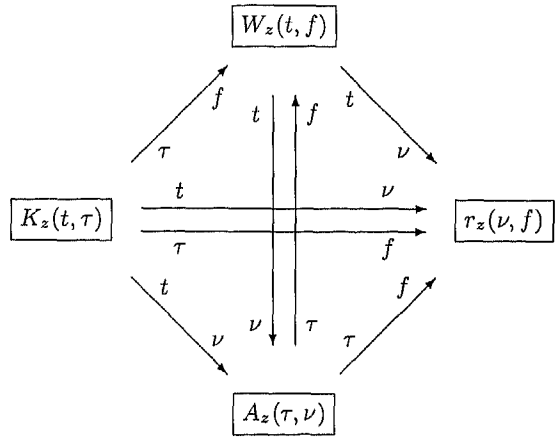

FIGURE 6.5. Different dual domain representations of signal $z(t)$, obtained from the signal kernel $K_z(t,\tau)$.

Given that a double convolution in (t, f) results, by 2D FT, in a multiplication in the ambiguity domain, $\mathcal{A}_z(\tau,\nu)$ becomes a windowed version of $A_z(\tau,\nu)$. This leads to the interpretation of TFD design, defined by Eq. (6.1.19), as a 2D filtering procedure in the ambiguity domain.

Equation (6.1.20) can therefore be rewritten as the 2D FT of the symmetric ambiguity function $A_z(\tau,\nu)$ filtered by the TFD kernel filter $g(\tau,\nu)$ [2]:

$$A_z(\tau,\nu)\, g(\tau,\nu) = \mathcal{A}_z(\tau,\nu) \overset{\tau}{\underset{\nu}{\rightleftharpoons}} \overset{f}{\underset{t}{}} \rho_z(t,f) = \int_{-\infty}^{\infty}\int_{-\infty}^{\infty} g(\tau,\nu) A_z(\tau,\nu) e^{j2\pi(\nu t - f\tau)} d\nu\, d\tau. \tag{6.1.25}$$

Choosing the kernel filter $g(\tau,\nu)$ in Eq. (6.1.25) most relevant to an application results in a specific TFD. For an all-pass filter, $g(\tau,\nu) = 1$, $\rho_z(t,f)$ reduces to the WVD. For $g(\tau,\nu)$ chosen to be the ambiguity function of a time analysis window $w(t)$, $\rho_z(t,f)$ corresponds to the spectrogram with window $w(t)$ [2,3].

6.1.5.4 Quadratic TFDs, multicomponent signals, and cross-terms reduction

Equation (6.1.20) defines TFDs that are quadratic (or bilinear) in the signal $z(t)$. This implies that if $z(t)$ includes two components $z_1(t)$ and $z_2(t)$, then its quadratic formulation will not only include these two components but also additional components corresponding to their cross product $z_1(t)\, z_2(t)$. These additional components are often called cross-terms and are considered as "artifacts" or "ghosts" appearing unexpectedly in the (t, f) representation. In Figure 6.6 (the WVD of two linear FMs), the "ghost" component is located halfway between the two signal components, and has an (oscillating) amplitude that exhibits large positive and negative values [3]. An effect similar to cross-terms appearance in (t, f) representations occurs when we

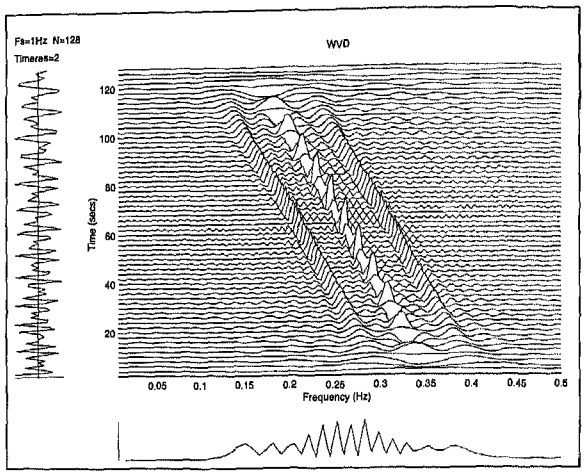

FIGURE 6.6. WVD of a signal composed of two linear FMs. The middle "component," exhibiting large positive and negative amplitudes, is known as the cross-term.

take the spectrum of $z_1(t)+z_2(t)$; we obtain cross-spectral components that are zero only when $z_1(t)$ and $z_2(t)$ do not overlap in frequency.

Thus, the introduction of either noise or some other deterministic components in $z(t)$ introduces cross-terms in its representations. In some applications the cross-terms may be useful, as they provide additional features that can be used for signal identification and recognition [6, Chapter 18]. However, in most cases, they are considered as undesirable interference terms that distort the reading of the representation. So it is generally desired to design TFDs that suppress them "best."

6.1.5.4.1 Location of cross-terms

It was shown that a signal mapped by $A_z(\tau,\nu)$ into the lag-Doppler domain always traverses the origin of that plane, while the cross-terms, having oscillating amplitude in the time-frequency domain, are located away from the origin in the lag-Doppler plane, the distance being directly proportional to the time and frequency separation of the signal components [2, Articles 4.2 and 5.1], [12]. This is illustrated in Figure 6.7 for a two-component signal whose (Gaussian-like) components are centered in the time-frequency domain at (t_1, f_1) and (t_2, f_2), respectively.

Since the WVD is related to the ambiguity function by a 2D FT (Eq. (6.1.25)), the simplest way to reduce the cross-terms of the WVD would be by filtering them out in the ambiguity domain, before taking a two-dimensional FT to return to the (t, f) domain. The two-dimensional filter $g(\tau,\nu)$ needs to be chosen such that it "passes" the region of the ambiguity plane close to the origin (where the signal components are located), and at the same time attenuates the rest of the plane. Note that any resulting truncation of the signal terms by the kernel filter $g(\tau,\nu)$ would result in the signal components spreading in the (t, f) domain, and so in the loss of their time-frequency resolution. So, a compromise is needed when defining the kernel filter in

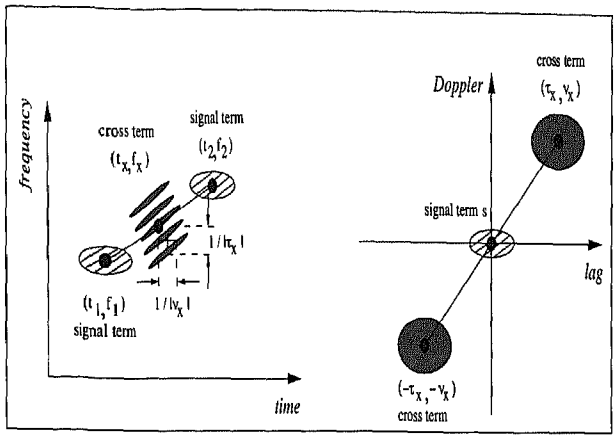

FIGURE 6.7. Location of signal terms and cross-terms in the (t, f), left, and (τ, ν), right, domain.

the ambiguity domain (and setting its parameters) such that the best possible trade-off is achieved between time-frequency resolution and cross-terms suppression.

6.1.5.4.2 Reduced interference TFDs

Many TFDs have been designed for the purpose of cross-terms suppression, the most popular among them belonging to the class of reduced interference distributions (RIDs) [6, 13]. One of the first RIDs was the Choi–Williams distribution (CWD), whose $g(\tau, \nu)$ is a 2D Gaussian function centered around the origin in the ambiguity plane, with its spread controlled by a parameter σ [13].

Another, more recent, reduced interference TFD is the MBD [5], whose time-lag kernel filter is defined as

$$G(t, \tau) = G(t) = \frac{k}{\cosh^{2\beta}(t)}, \tag{6.1.26}$$

where $k = \Gamma(2\beta)/(2^{2\beta-1}\Gamma^2(\beta))$ is the normalizing factor ($\Gamma(\cdot)$ stands for the gamma function), and β is a real, positive number that controls the sharpness of the cutoff of the kernel filter in the ambiguity domain, and so also controls the trade-off between time-frequency resolution and cross-terms suppression.

The MBD was found to be the closest to the ideal compromise; it is almost cross-terms free and has high components' resolution in the time-frequency plane [5]. In addition, the MBD allows an efficient IF estimation for multicomponent signals [5]. The original B distribution (BD) [14] also performs well, but it does not meet the traditional RIDs requirements. Both the BD and MBD are practically "equivalent" to the WVD in the analysis and estimation of a monocomponent linear FM signal [5, 14].

6.1.5.4.3 Reduced interference TFDs with separable kernel filters

A simple way to achieve a good cross-terms suppression, and at the same time preserve the signal components' time-frequency resolution, is to design a TFD using a *separable* kernel filter expressed as

$$g(\tau,\nu) = g_2(\tau)\, G_1(\nu). \tag{6.1.27}$$

This product form allows us to formulate separate filter constraints for each variable.

A TFD corresponding to the separable kernel filter $g(\tau,\nu)$ is then defined, using Eq. (6.1.20), as

$$\rho_z(t,f) = g_1(t) \star_t W_z(t,f) \star_f G_2(f), \tag{6.1.28}$$

where $g_1(t) = \underset{\nu\to t}{\mathcal{F}}^{-1}\{G_1(\nu)\}$ and $G_2(f) = \underset{\tau\to f}{\mathcal{F}}\{g_2(\tau)\}$.

Separable kernel filters, therefore, allow for separate convolutions of the WVD in both time and frequency directions. This makes the design of such TFDs easier to implement. Note that the (t,f) domain form of the separable kernel filter $g(\tau,\nu)$ is also a separable kernel filter $\gamma(t,f) = g_1(t)G_2(f)$ [2].

Two special subclasses of separable kernel filters are:

- the Doppler-independent ($G_1(\nu) = 1$) kernel filters, which allow for smoothing of the WVD in the frequency direction only, and
- the lag-independent ($g_2(\tau) = 1$) kernel filters, which allow for the WVD smoothing in the time direction only.

The properties of the Doppler-independent and the lag-independent kernel filters are studied in detail in [2, Article 5.7].

For the WVD of a multicomponent signal, the inner interference terms [3] resulting from a nonlinear FM law of the signal components alternate in the frequency direction, so they can be successfully suppressed by a Doppler-independent kernel filter [2, Article 5.7]. The cross-terms of the WVD oscillate in the time direction [3], and so they can be significantly suppressed by filtering the WVD with a time window, which is the inverse FT of a lag-independent kernel filter [2, Article 5.7]. To successfully suppress both types of these interfering terms in the WVD of a multicomponent signal, a full *separable* kernel filter can be used.

The BD kernel filter [14], $g(\tau,\nu) = (|\tau|/\cosh^2(t))^\beta$, is an example of separable kernels. It was shown in [14] that, for small values (close to zero) of its parameter β, this TFD in general performs well for different types of signals. For small values of β, the BD kernel can be approximated by the lag-independent kernel filter $g_1(t) = 1/\cosh^{2\beta}(t)$ [2, Article 5.7], which, when normalized, defines the MBD kernel filter (see Eq. (6.1.26)). The MBD achieves in particular good cross-terms suppression and good resolution of closely spaced components of multicomponent signals when the components have slowly varying IF laws, as shown in [2, Article 5.7], and illustrated by several examples in this chapter. The definitions and properties of other classical and popular quadratic TFDs are provided in [2].

For a more conclusive assessment of the relative worth of each TFD, a quantitative comparison of their performance is needed. This requires the introduction of specific criteria that take into account usual key attributes of TFDs (such as the amplitudes of signal components and cross-terms, components' instantaneous bandwidths, sidelobes' amplitudes, etc.) [1], as detailed in the next section.

6.2 Performance assessment for quadratic TFDs

6.2.1 Visual comparison of TFDs

Stationary signals are usually analyzed and compared in either the time or the frequency domain. The autocorrelation function in time is examined by looking at the position and relative amplitudes of each lobe, as well as the "correlation width" of the mainlobe. These characteristics are used for examination and comparison. The PSD in frequency is examined by looking at the position and relative amplitude of spectral peaks. It is desired to resolve closely located spectral peaks in the PSD.

For nonstationary signals with a time-varying spectrum, TFSP techniques are needed to represent the signals in the joint time-frequency domain using an appropriate choice of TFD.

Just as some spectral estimates are better than others, some TFDs outperform others when used to analyze certain classes of signals [3, 15–17]. For example, the WVD is known to be optimal for monocomponent signals with the quadratic phase law (linear frequency modulation (LFM)), since it achieves the best energy concentration around the signal IF law [2,3] (see Figure 6.3). The spectrogram, on the other hand, although still regarded as one of the most popular quadratic TFDs, results in an undesirable smoothing of the signal energy around its IF [3].

This example is just a simple illustration of the fact that choosing the right TFD to analyze the given signal is not straightforward, even for monocomponent signals. The task, then, appears to be more complex when one deals with multicomponent signals.

For illustration, let us consider a multicomponent bird song signal [18], represented in the (t, f) domain using the Born–Jordan distribution [2], the CWD, the MBD, the Rihaczek distribution [10], the smoothed WVD [3, 6], the spectrogram, the WVD, and the Zhao–Atlas–Marks distribution [19] (Figure 6.8).

How do we determine which of the TFDs in Figure 6.8 best represents the given signal? To answer this question, according to the common practice in TFSP, one would *visually* compare the eight plots and choose the one that is most appealing. From Figure 6.8, we can see that the MBD, the smoothed WVD, and the spectrogram have "cleaner" plots (less interference, better components' concentration) than the other considered TFDs. However, selecting the best time-frequency distribution among those three TFDs, based *only* on the visual comparison of their plots, is difficult.

The need to *objectively* compare the plots in Figure 6.8 requires the definition of a quantitative performance measure for TFDs. Some theoretical measures that deal

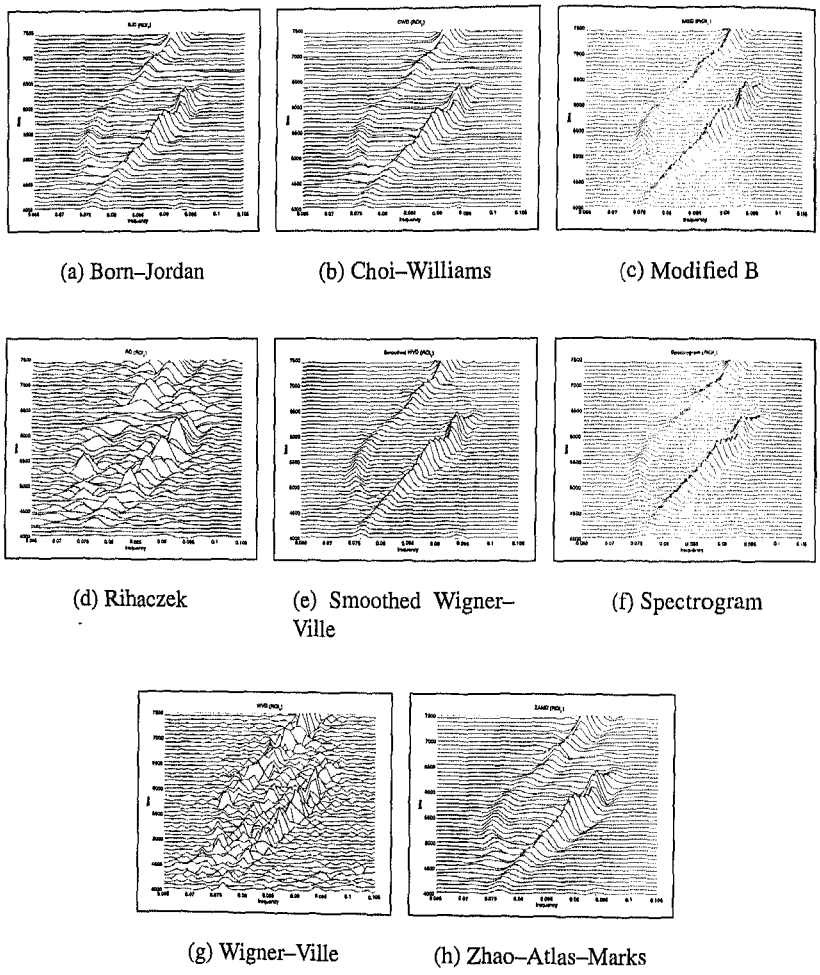

(a) Born–Jordan (b) Choi–Williams (c) Modified B

(d) Rihaczek (e) Smoothed Wigner–Ville (f) Spectrogram

(g) Wigner–Ville (h) Zhao–Atlas–Marks

FIGURE 6.8. TFDs of a multicomponent bird song signal.

essentially with signal concentration have been proposed in the literature [20–23]. This chapter uses objective quantitative measure criteria that take into account not only concentration but also resolution aspects for a practical analysis in the case of closely spaced components. The characteristics of TFDs that influence their resolution, such as energy concentration, mainlobes separation, and sidelobes and cross-terms minimization, need to be combined to define these quantitative measure criteria, as explained in the following section.

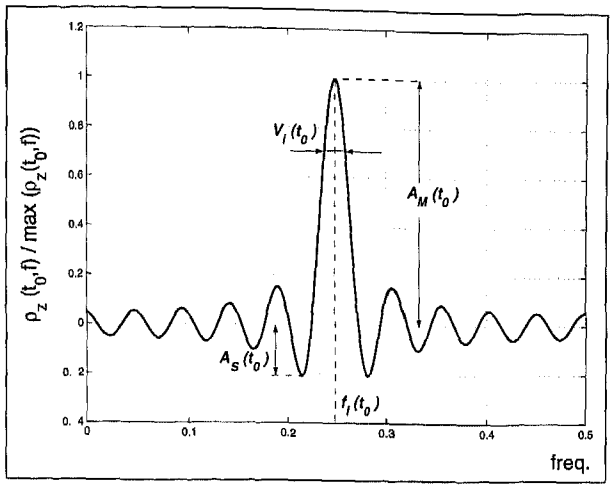

FIGURE 6.9. Instantaneous ($t = t_0$) TFD resolution performance for a monocomponent FM signal.

6.2.2 *Performance criteria for TFDs*

6.2.2.1 Monocomponent signal

For a *monocomponent* FM signal, performance of its TFD is usually defined in terms of the energy concentration that the TFD achieves about the signal IF [4]. One desires to minimize sidelobe amplitude $A_S(t)$ relative to mainlobe amplitude $A_M(t)$, and to minimize instantaneous (mainlobe) bandwidth $V_i(t)$ about the signal IF $f_i(t)$.

For a given time slice of a TFD of a monocomponent signal, as illustrated in Figure 6.9, we may then quantify the signal TFD performance by the measure p expressed as

$$p(t) = \left| \frac{A_S(t)}{A_M(t)} \right| \frac{V_i(t)}{f_i(t)}. \tag{6.2.1}$$

For clarity of presentation, we limit ourselves to measuring the instantaneous bandwidth at 0.7071 of the component normalized amplitude. Note also that in Eq. (6.2.1) we have normalized the bandwidth $V_i(t)$ with the IF $f_i(t)$. However, other possible normalization factors are currently being studied, such as the signal sampling frequency, or the signal half-power bandwidth [11].

From Eq. (6.2.1), good performance of a TFD is characterized by a small (close to zero) value of its measure p. The WVD of an LFM signal with infinite duration, for example, has $p = 0$ [2, Article 7.4].

6.2.2.2 Multicomponent signal

For a *multicomponent* FM signal, performance of its TFD involves not only the energy concentration the TFD attains about the respective IFs of each component,

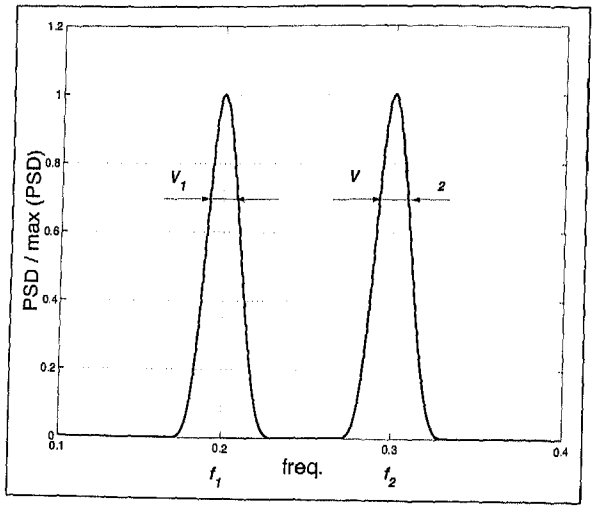

FIGURE 6.10. PSD estimate resolution performance for two sinusoids.

but also the resolution, as measured by the minimum frequency separation between the components' mainlobes for which their amplitudes and bandwidths are just preserved. Let us define these two notions.

6.2.2.2.1 *Energy concentration*

By extending the concept introduced in Subsection 6.2.2.1 for a monocomponent signal, we say that a TFD has best energy concentration for a given multicomponent signal if *for each* signal component it yields the smallest:

- instantaneous bandwidth relative to the component IF $(V_i(t)/f_i(t))$,
- sidelobe magnitude relative to mainlobe magnitude $(|A_S(t)/A_M(t)|)$.

6.2.2.2.2 *Resolution*

The frequency resolution in a PSD estimate of a signal composed of two single tones, f_1 and f_2, is defined as the minimum difference $f_2 - f_1$ for which the following inequality holds:

$$f_1 + \frac{V_1}{2} < f_2 - \frac{V_2}{2}, \qquad f_1 < f_2, \tag{6.2.2}$$

where V_1 and V_2 are the bandwidths of the first and the second sinusoid, respectively, as illustrated in Figure 6.10.

For most quadratic TFDs of a two-component signal, however, we also need to account for the effect of cross-terms on resolution, as illustrated by Figure 6.11. From Figure 6.11, we can see that in order to make Eq. (6.2.2) applicable to TFD slices, TFDs should first minimize the cross-terms relative to signal components. Therefore,

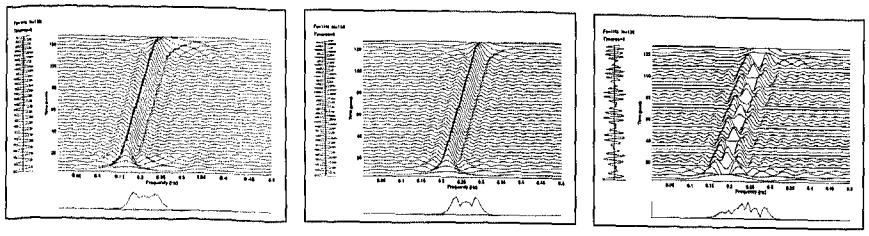

(a) WVD of the first component

(b) WVD of the second component

(c) WVD of the sum

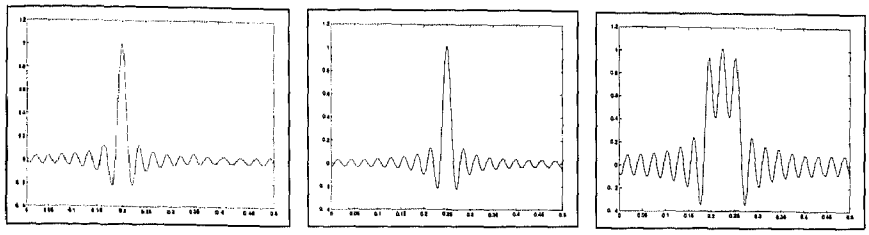

(d) Slice of (a)

(e) Slice of (b)

(f) Slice of (c)

FIGURE 6.11. WVD (a–c) and its slice at the middle of the signal duration interval (d–f) for a two-component signal, considered individually for each contributing term and combined.

the concentration requirement for each signal component needs to be complemented by the cross-term suppression requirement when evaluating the resolution performance of TFDs. All important signal parameters that are needed for this purpose are shown in Figure 6.12, which represents a time slice ($t = t_0$) of a typical quadratic TFD.

In Figure 6.12, $V_{i_1}(t_0)$, $f_{i_1}(t_0)$, $A_{S_1}(t_0)$ and $A_{M_1}(t_0)$ denote, respectively, the instantaneous bandwidth, the IF, the sidelobe amplitude, and the mainlobe amplitude of the first component at time $t = t_0$. Similarly, $V_{i_2}(t_0)$, $f_{i_2}(t_0)$, $A_{S_2}(t_0)$, and $A_{M_2}(t_0)$ represent the instantaneous bandwidth, the IF, the sidelobe amplitude, and the mainlobe amplitude of the second component at the same time t_0. $A_X(t_0)$ is the cross-terms amplitude.

An example of a TFD with nonresolved components is shown in Figure 6.13, where the signal components and the cross-term have all merged in a single lobe.

6.2.2.3 Resolution performance measure for quadratic TFDs

From Eq. (6.2.2) and Figure 6.12, the frequency resolution of a TFD for a pair of components in a multicomponent signal may be quantified by the minimum difference $f_{i_2}(t) - f_{i_1}(t)$ ($f_{i_1}(t) < f_{i_2}(t)$) for which a separation measure D between the

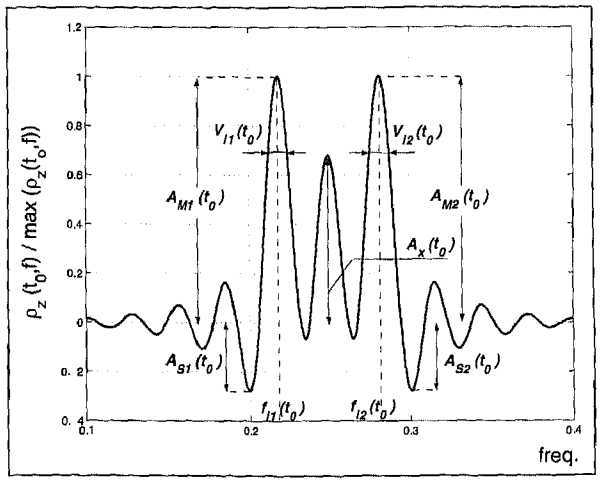

FIGURE 6.12. Instantaneous ($t = t_0$) TFD resolution performance for a two-component FM signal with *resolved* components.

components' mainlobes, centered about their respective IFs f_{i_2} and f_{i_1}, is positive. We define the components' separation measure D as

$$D(t) = \frac{(f_{i_2}(t) - V_{i_2}(t)/2) - (f_{i_1}(t) + V_{i_1}(t)/2)}{f_{i_2}(t) - f_{i_1}(t)}$$
$$= 1 - \frac{1}{2}\left(\frac{V_{i_1}(t) + V_{i_2}(t)}{f_{i_2}(t) - f_{i_1}(t)}\right). \tag{6.2.3}$$

For a better resolution performance of quadratic TFDs:

- the separation measure D should be maximized (close to 1), and *concurrently*,
- the interfering terms (cross-terms and components' sidelobes) should be minimized.

To maximize D, we need to maximize the energy concentration for each component in a pair of signal components under analysis by minimizing their instantaneous bandwidths about the components IFs.

The interfering terms, on the other hand, can be minimized by minimizing both the sidelobe–mainlobe amplitude ratio $|A_S(t)/A_M(t)|$ (so also improving the energy concentration) for each component, and the cross-term—components' mainlobe amplitudes ratios $|A_X(t)/A_M(t)|$.

Therefore, an overall measure P of the resolution performance of a TFD for a pair of components in a multicomponent signal can then be expressed as [1]

$$P(t) = \left|\frac{A_S(t)}{A_M(t)}\right| \left|\frac{A_X(t)}{A_M(t)}\right| \frac{1}{D(t)}, \tag{6.2.4}$$

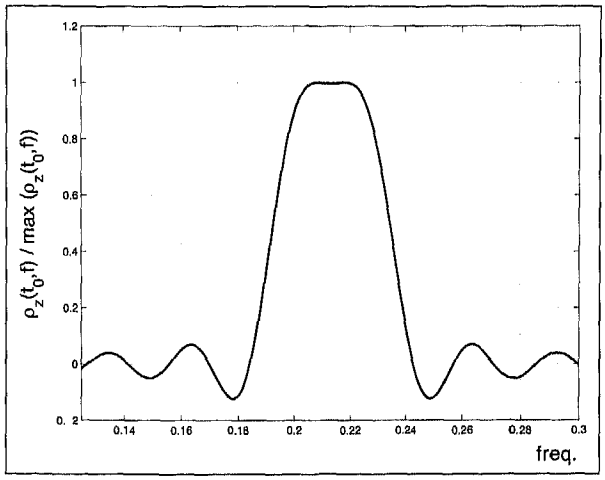

FIGURE 6.13. Instantaneous ($t = t_0$) TFD resolution performance for a two-component FM signal with *unresolved* components.

where $A_M(t)$, $A_S(t)$, and $A_X(t)$ are, respectively, the average amplitude of the components' mainlobes, the average amplitude of the components' sidelobes, and the cross-term amplitude, and $D(t)$, defined by Eq. (6.2.3), is a measure of the components' separation in frequency.

From Eq. (6.2.4) we can see that a good resolution performance of a TFD for a given pair of components in a multicomponent signal is characterized by a small (close to zero) positive value of the measure P.

6.2.2.4 Assessment of the resolution performance of TFDs for a two-LFM-component signal

As an illustration of the use of the performance measure P in Eq. (6.2.4), let us consider a multicomponent signal $s_1(t)$ of duration $T = 128$ given by

$$s_1(t) = \cos\left(2\pi(0.15\,t + 0.0004\,t^2)\right) + \cos\left(2\pi(0.2\,t + 0.0004\,t^2)\right). \qquad (6.2.5)$$

The signal $s_1(t)$ is represented in the time-frequency domain using a selection of TFDs (see Figure 6.14). In this example, we compare the TFDs' resolution performance at the middle of the signal duration interval. So, for each TFD we take a slice at $t = 64$ and measure the parameters $A_M(64)$, $A_S(64)$, $A_X(64)$ and $V_i(64)$ (the average of the components' instantaneous bandwidths). Using these, we then calculate the frequency separation measure of the components $D(64)$, defined by Eq. (6.2.3), and the resolution performance measure $P(64)$, defined by Eq. (6.2.4). The measurements results are recorded in Table 6.1, and the slices of the TFDs at $t = 64$ are shown in Figure 6.15.

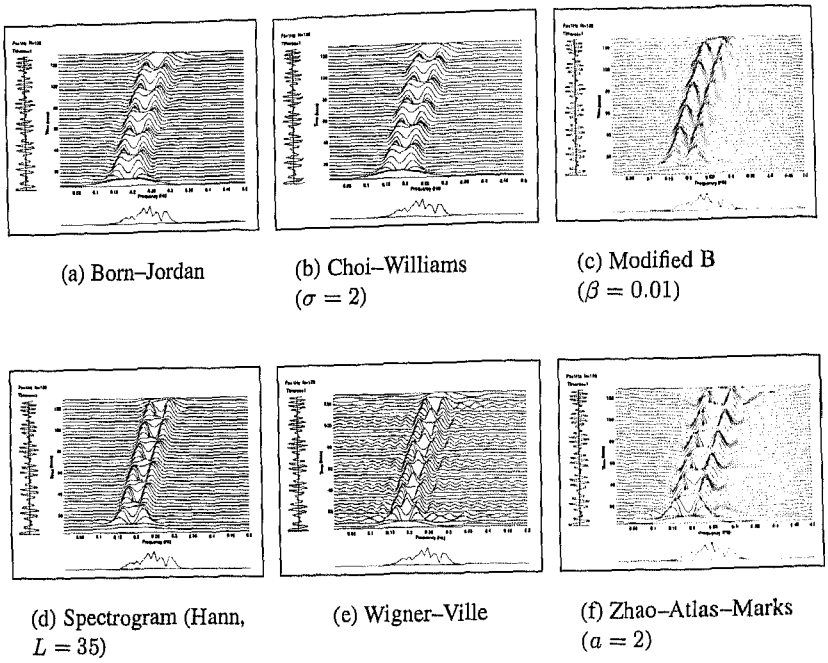

(a) Born–Jordan

(b) Choi–Williams ($\sigma = 2$)

(c) Modified B ($\beta = 0.01$)

(d) Spectrogram (Hann, $L = 35$)

(e) Wigner–Ville

(f) Zhao–Atlas–Marks ($a = 2$)

FIGURE 6.14. TFDs of signal $s_1(t)$ defined by Eq. (6.2.5).

As indicated by Eq. (6.2.4), a TFD that, at a given time instant, has the smallest positive value of the measure P is the TFD with the best resolution performance at that time instant for the signal under analysis. From Table 6.1, the MBD ($\beta = 0.01$) of signal $s_1(t)$ gives the smallest value for P at time $t = 64$, and hence should be selected as the best-performing TFD of $s_1(t)$ at $t = 64$.

TFD	$A_M(64)$	$A_S(64)$	$A_X(64)$	$V_i(64)$	$D(64)$	$P(64)$
Born–Jordan	0.9320	0.1222	0.3798	0.0219	0.5512	0.0969
Choi–Williams	0.9355	0.0178	0.4415	0.0238	0.5174	0.0174
Modified B	0.9676	0.0099	0.0983	0.0185	0.6483	0.0016
Spectrogram	0.9119	0.0087	0.5527	0.0266	0.5309	0.0109
Wigner–Ville	0.9153	0.3365	1	0.0130	0.7735	0.5193
Zhao–Atlas–Marks	0.9146	0.4847	0.4796	0.0214	0.4905	0.5666

TABLE 6.1. Parameters and the resolution performance measure P of the signal $s_1(t)$ (Eq. (6.2.5)) TFDs' slices, shown in Figure 6.15.

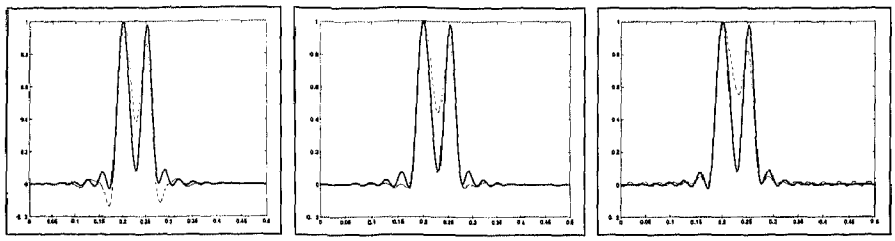

(a) Modified B (solid), Born–Jordan (dashed)

(b) Modified B (solid), Choi–Williams (dashed)

(c) Modified B (solid), Spectrogram (dashed)

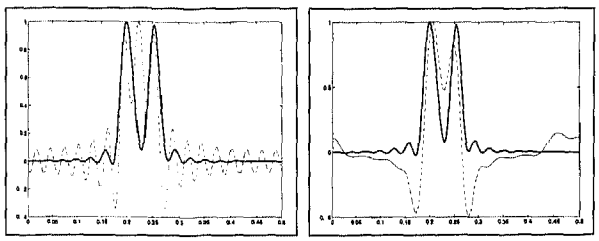

(d) Modified B (solid), Wigner–Ville (dashed)

(e) Modified B (solid), Zhao–Atlas–Marks (dashed)

FIGURE 6.15. Normalized slices of TFDs plotted in Figure 6.14 taken at a half of the time interval ($t = 64$) of signal $s_1(t)$ (Eq. (6.2.5)).

6.2.2.5 Alternative (normalized) resolution performance measure

An alternative to the measure P, defined by Eq. (6.2.4), is to combine $|A_S(t)/A_M(t)|$, $|A_X(t)/A_M(t)|$, and $D(t)$ into a sum, rather than a product, and so account for their effects more independently. This results in the following definition for the resolution performance measure [24]:

$$P_1(t) = \left|\frac{A_S(t)}{A_M(t)}\right| + \left|\frac{A_X(t)}{A_M(t)}\right| + \frac{1}{D(t)}. \tag{6.2.6}$$

We would like to have a performance measure that is close to one for TFDs that perform well, and close to zero for poor-performing ones. This requires P_1 to be normalized, for which we need to normalize each of its three contributing terms.

Since, from Eq. (6.2.3), $0 < D(t) < 1$ for resolved components, and therefore $1 < 1/D(t) < \infty$ cannot be normalized, we have chosen to use $(1 - D(t))$ instead of $1/D(t)$ in Eq. (6.2.6). Note that we want to minimize $0 < (1 - D(t)) < 1$ in order to achieve good frequency separation of signal components.

On the other hand, the sidelobe magnitude $|A_S(t)|$ will always be smaller than the mainlobe magnitude $|A_M(t)|$, while the cross-term magnitude $|A_X(t)|$ can be as

large as twice the magnitude of the signal components [3] (we assume here normalized amplitudes). Therefore,

$$0 < \left|\frac{A_S(t)}{A_M(t)}\right| < 1, \quad \text{and} \quad 0 < \frac{1}{2}\left|\frac{A_X(t)}{A_M(t)}\right| < 1. \tag{6.2.7}$$

By combining the three normalized quantities into a sum, and normalizing this sum, another resolution performance measure P_2 is obtained [24]:

$$P_2(t) = \frac{1}{3}\left\{\left|\frac{A_S(t)}{A_M(t)}\right| + \frac{1}{2}\left|\frac{A_X(t)}{A_M(t)}\right| + (1 - D(t))\right\}, \tag{6.2.8}$$

where the scaling factor $1/3$ normalizes the summation.

Smaller values of P_2 mean better resolution performance of TFDs. To make this measure be close to 1 for well-performing TFDs and 0 for poor-performing ones (TFDs with large interfering terms and poorly resolved components), we have defined the *normalized instantaneous resolution performance measure* P_i as [2, Article 7.4]

$$P_i(t) = 1 - \frac{1}{3}\left\{\left|\frac{A_S(t)}{A_M(t)}\right| + \frac{1}{2}\left|\frac{A_X(t)}{A_M(t)}\right| + (1 - D(t))\right\}, \quad 0 < P_i(t) < 1. \tag{6.2.9}$$

6.2.3 *Performance specifications for the design of high resolution TFDs*

In order to design TFDs that behave optimally in the difficult case of closely spaced multicomponent signals, we need to revisit the constraints for TFD design, discussed in Subsection 6.1.4.2.3, and relate them to the performance measure P_i defined by Eq. (6.2.9).

Subsection 6.1.4.2.3 lists five properties. The first two ensure a physical interpretation of TFDs (i.e., energy conservation), while the last two directly relate to the performance measure P_i. The third property ensures that the IF peak requirement is verified. So, these five properties could be further reduced to essentially three combined ones.

Following this logic, to be a suitable tool for a *practical* high resolution time-frequency analysis, a TFD must verify the following properties:

1. Preserve and concentrate signal energy (Properties P1 and P2 of Subsection 6.1.4.2.3)
2. Reveal the IF law(s) of a signal by its peak(s) (Property P3 of Subsection 6.1.4.2.3)
3. Maximize the measure P_i, defined by Eq. (6.2.9), in order to reduce the cross-terms while preserving time-frequency resolution and improving noise performance (Properties P4 and P5 of Subsection 6.1.4.2.3).

In order to define a quadratic TFD that best meets these constraints, we could use the separable kernel TFD design procedure of Subsection 6.1.5.4.3, and then vary the windows $G_1(\nu)$ and $g_2(\tau)$ until the value of the performance measure P_i is maximum for a given class of signals.

One outcome of such a procedure is the MBD [5], whose kernel filter is defined by Eq. (6.1.26). The kernel filter of the MBD was chosen in the ambiguity domain to be a 2D low-pass function centered around the origin, with sharp cutoff edges. In this way, the kernel retains as much of the auto-terms as possible, while attenuating cross-terms. The amounts of auto-terms and cross-terms kept and filtered out are functions of the volume underneath the kernel filter $g(\tau, \nu)$. This volume can be changed by varying the parameter β.

The MBD and its original version the BD, meet the properties listed above, although, like the spectrogram, they do not satisfy the marginals [5, 14, 25].

6.3 Selecting the best TFD for a given practical application

6.3.1 Assessment of performance for selection of the best TFD

6.3.1.1 Assessment and selection procedure

The procedure for selecting the optimal time-frequency representation for a given multicomponent signal consists of the following steps:

1. *Define a set of criteria for comparison of TFDs*: The criteria must be related to the information we seek from a TFD (e.g., the number of signal components, their relative amplitudes, components' frequency modulation laws, etc.). A set of such criteria is defined in Subsection 6.2.2 for both mono- and multicomponent signals.
2. *Define a quantitative measure for evaluating TFDs performance based on these criteria*: The measure P_i (Eq. (6.2.9)), for example, has been defined for evaluating the resolution performance of quadratic TFDs based on the comparison criteria for FM signals described in Subsection 6.2.2.
3. *Optimize TFDs to match the comparison criteria as closely as possible*: The optimization procedure for a TFD with parameter α (e.g., MBD with parameter β, or CWD with parameter σ) can be done as follows. First, we choose the initial value for the parameter α (a value closest to its lower bound) and calculate the TFD of a given signal. For each time instant in the time interval of interest (time instants over which we want to compare the performance of different TFDs), we take a slice of the TFD and measure its instantaneous performance (e.g., use P_i defined by Eq. (6.2.9)). The average of all instantaneous measures defines the interval performance measure of the TFD for the given value of α.
   The procedure is repeated for the next value of the parameter α. The increment in α should be neither too small (long computation time) nor too large (too "coarse"

optimization results). The optimal value of the parameter α is that value of α that maximizes the TFD interval performance measure. This maximum value of the TFD interval performance measure is called the TFD optimal performance measure.

4. *Select the best TFD for the given signal*: When all TFDs used to represent the given signal in the joint (t, f) domain are optimized, the TFD with the largest value of its optimal performance measure is selected as the *best* TFD for the analyzed signal.

6.3.1.2 Resolution performance comparison of TFDs for a two-LFM-component signal in additive white Gaussian noise

The following example illustrates how to use the above procedure for selecting the optimal TFD for the two-component signal $s_1(t)$ (Eq. (6.2.5)) embedded in noise, i.e.,

$$s_2(t) = \cos\left(2\pi(0.15\,t + 0.0004\,t^2)\right) + \cos\left(2\pi(0.2\,t + 0.0004\,t^2)\right) + n(t), \tag{6.3.1}$$

where $n(t)$ is additive white Gaussian noise, with a signal-to-noise ratio (SNR) of 10 dB.

The signal $s_2(t)$, of duration $T = 128$, is analysed in the (t, f) domain using the Born–Jordan distribution, the CWD, the MBD, the spectrogram, the WVD, and the Zhao–Atlas–Marks distribution.

To find the TFD that best resolves the two LFM components of the signal $s_2(t)$, we first optimize each of the considered TFDs, as defined in step 3 of the procedure in Subsection 6.3.1.1 (note that the WVD and the Born–Jordan distribution (α [2] equals $1/2$, by convention) have no kernel filter parameters, and hence need no optimizing). The resolution performance of TFDs is compared based on the criteria defined in Subsection 6.2.2, using the comparison measure P_i (Eq. (6.2.9)). The optimal resolution performance measure, P_{opt}, is found for each of the TFDs. Table 6.2 contains the results of the optimization process. It shows that the optimal TFD for signal $s_2(t)$ is the MBD with parameter $\beta = 0.002$, as it has the largest value of P_{opt}. The time-frequency plots of the optimized TFDs are shown in Figure 6.16.

TFD	*Optimal kernel filter parameter*	P_{opt}
Born–Jordan	N/A	0.7542
Choi–Williams	$\sigma = 0.5$	0.7976
Modified B	$\beta = 0.002$	0.8605
Spectrogram	Bartlett window, length 47	0.8448
Wigner–Ville	N/A	0.6694
Zhao–Atlas–Marks	$a = 8$	0.6550

TABLE 6.2. Optimization results for TFDs of signal $s_2(t)$ defined by Eq. (6.3.1).

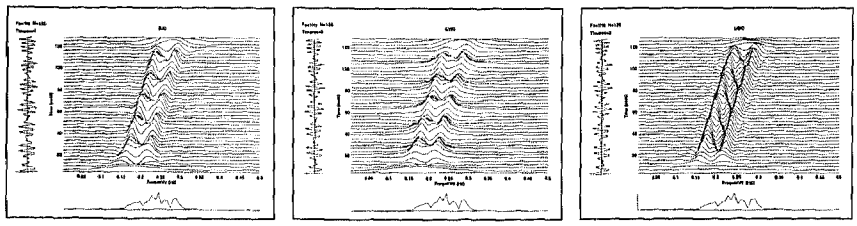

(a) Born–Jordan

(b) Choi–Williams ($\sigma = 0.5$)

(c) Modified B ($\beta = 0.002$)

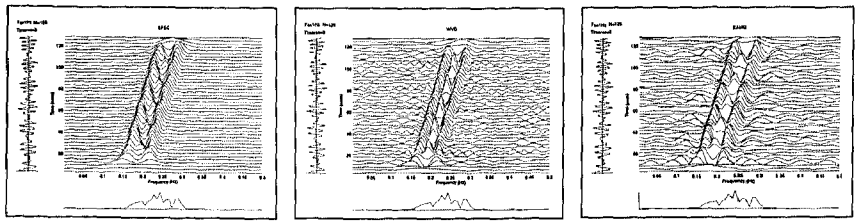

(d) Spectrogram (Bart, $L = 47$)

(e) Wigner–Ville

(f) Zhao–Atlas–Marks ($a = 8$)

FIGURE 6.16. Optimised TFDs of signal $s_2(t)$ defined by Eq. (6.3.1).

As explained in Subsections 6.1.4.2.3 and 6.2.3, for a practical time-frequency analysis, an important property that a TFD should satisfy is to accurately reveal the IF laws of signal components by its peaks. In Figure 6.17 we compare the true IF laws of the two signal components with those measured from the peaks of the optimized MBD (the best-performing TFD for $s_2(t)$), and the optimized spectrogram (second best TFD for $s_2(t)$).

The quality of the components' IF estimates is measured using the mean-squared error (MSE). As indicated by the MSE values, recorded in Figure 6.17 next to each of the two components, the MBD provides more accurate estimates (smaller MSEs) than the spectrogram for *both* components of the noisy two-component signal $s_2(t)$.

6.3.1.3 Resolution performance comparison of TFDs for a signal with a linear and a nonlinear FM component embedded in additive white Gaussian noise

The optimal TFD methodology is now illustrated for a two-component signal $s_3(t)$ comprising a quadratic FM component whose frequency varies from 0.1 Hz to 0.3 Hz (the sampling frequency is $f_s = 1$ Hz) over the time interval $t \in [1, 128]$, and a component that linearly decreases in frequency from 0.4 Hz to 0.275 Hz over the

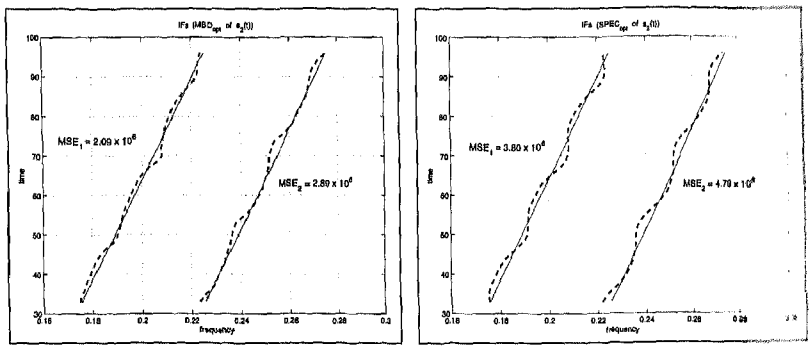

(a) Modified B: $MSE_1 = 2.09 \times 10^{-6}$, $MSE_2 = 2.89 \times 10^{-6}$

(b) Spectrogram: $MSE_1 = 3.80 \times 10^{-6}$, $MSE_2 = 4.79 \times 10^{-6}$

FIGURE 6.17. Comparison of the measured (dashed) and true (solid) IF laws of the two linear FM components of signal $s_2(t)$, defined by Eq. (6.3.1), for the optimized MBD (a) and the optimized spectrogram (b) of $s_2(t)$.

same time interval but has nonzero rectangular amplitude values only for $t \in [33, 96]$. A diagram illustrating the IF laws of the signal $s_3(t)$ is shown in Figure 6.18.

We measure the optimized performance P_{opt} of the Born–Jordan, Choi–Williams, Modified B, spectrogram, Wigner–Ville, and Zhao–Atlas–Marks distributions, when these TFDs represent $s_3(t)$ in the joint time-frequency domain. Table 6.3 lists the TFDs' optimal performance measures and the corresponding optimal values of their kernel filter parameters. It shows that the signal best-performing TFD is the spectrogram ($P_{opt} = 0.84$), closely followed by the MBD ($P_{opt} = 0.8361$).

If we repeat this experiment, but embed the signal $s_3(t)$ in additive white Gaussian noise for two different values of SNR, then:

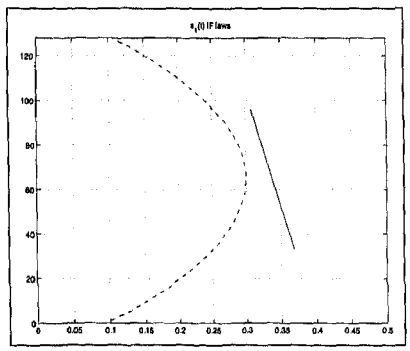

FIGURE 6.18. Diagram illustrating the IF laws of signal $s_3(t)$.

TFD	*Optimal kernel filter parameter*	P_{opt}
Born–Jordan	N/A	0.7114
Choi–Williams	$\sigma = 0.7$	0.7660
Modified B	$\beta = 2.6 \times 10^{-3}$	0.8361
Spectrogram	Hamming window, length 53	0.8400
Wigner–Ville	N/A	0.6232
Zhao–Atlas–Marks	$a = 7$	0.6359

TABLE 6.3. Optimization results for TFDs of signal $s_3(t)$.

TFD	*Optimal kernel filter parameter*	P_{opt}
Born–Jordan	N/A	0.7073
Choi–Williams	$\sigma = 0.5$	0.7414
Modified B	$\beta = 7 \times 10^{-3}$	0.8316
Spectrogram	Bartlett window, length 57	0.8401
Wigner–Ville	N/A	0.5791
Zhao–Atlas–Marks	$a = 7$	0.6471

TABLE 6.4. Optimization results for TFDs of signal $s_3(t)$ in 5 dB additive white Gaussian noise.

TFD	*Optimal kernel filter parameter*	P_{opt}
Born–Jordan	N/A	0.6548
Choi–Williams	$\sigma = 45$	0.5811
Modified B	$\beta = 2.6 \times 10^{-3}$	0.8219
Spectrogram	Hanning window, length 47	0.7955
Wigner–Ville	N/A	0.5647
Zhao–Atlas–Marks	$a = 2$	0.5703

TABLE 6.5. Optimization results for TFDs of signal $s_3(t)$ in 0 dB additive white Gaussian noise.

1. For SNR = 0 dB, the optimal TFD is found to be the MBD, whose optimal resolution performance measure is $P_{opt} = 0.8219$. The spectrogram is the second best TFD with $P_{opt} = 0.7955$. Figure 6.19 shows the plots of the TFDs of signal $s_3(t)$ in 0 dB additive white Gaussian noise.
2. For SNR = 5 dB, the optimal TFD is the spectrogram ($P_{opt} = 0.8401$), while the MBD is the second best TFD ($P_{opt} = 0.8316$).

The performance of other TFDs for $s_3(t)$ in 5 and 0 dB noise is shown in Tables 6.4 and 6.5, respectively.

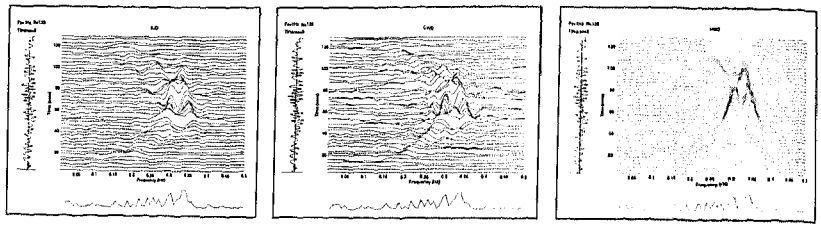

(a) Born–Jordan (b) Choi–Williams ($\sigma = 45$) (c) Modified B ($\beta = 0.0026$)

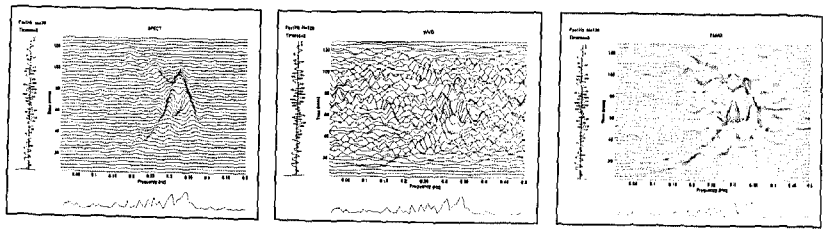

(d) Spectrogram (Hann, $L = 47$) (e) Wigner–Ville (f) Zhao–Atlas–Marks ($a = 2$)

FIGURE 6.19. Optimized TFDs of signal $s_3(t)$, with the components' IF laws defined in Figure 6.18, embedded in 0 dB additive white Gaussian noise.

The optimized spectrogram and the optimized MBD of signal $s_3(t)$ perform (out and in noise) similarly, with both TFDs clearly outperforming all other considered TFDs. In situations when two or more TFDs have similar performance for a given signal, the final choice of the signal's optimal TFD should be based on application-specific constraints, so that the TFD that more closely meets these constraints is selected as best over the other "optimal" TFD(s). For example, we have seen that the MBD and the spectrogram have similar resolution performance for the signal $s_2(t)$. However, if, in addition to the resolution requirement, the peak IF criterion (defined in Subsection 6.2.3) is considered, the MBD outperforms the spectrogram, and hence is selected as the optimal TFD for $s_2(t)$. The issue of selecting the optimal TFD under given constraints is further discussed, and illustrated on a real-life signal example, in Subsection 6.3.2.

6.3.1.4 Testing the resolution performance of TFDs for a three-component signal with *different frequency separation* between the components

We now compare the resolution performance of TFDs of a signal with *three* frequency components, with different separations between its consecutive components

in the time-frequency plane. The measure P_i, defined by Eq. (6.2.9), evaluates the TFD performance for a given pair of the signal components.

For this test, it suffices to consider a signal $s_4(t)$, which is a sum of three sinusoids: $f_1 = 0.1$ Hz, $f_2 = 0.2$ Hz, and $f_3 = 0.4$ Hz, all three defined over $t \in [1, 128]$. We define P_{i_1} to be the resolution performance measure for the first pair of components $\{f_1, f_2\}$ (closer components), and P_{i_2} the resolution performance measure of the second pair $\{f_2, f_3\}$ (more separated components). Table 6.6 shows the values of $P_{i_1}(64)$ and $P_{i_2}(64)$ for the Born–Jordan, Choi–Williams, Modified B, spectrogram, and Zhao–Atlas–Marks distributions. We do not consider the WVD in this example since the cross-terms significantly degrade its performance whenever there are more than two components in the signal.

Table 6.6 indicates that the MBD is the best-performing TFD for the pair of closer components, followed by the spectrogram, Choi–Williams, Born–Jordan, and Zhao–Atlas–Marks distributions. The *same* ranking of the considered TFDs is obtained for the pair of more separated components.

Thus, for signals with more than two components, we only need to determine a TFD's resolution performance measure for the pair of closest components. This value of the performance measure provides an indication of the TFD's resolution performance, with respect to other TFDs, for all other pairs of consecutive (in frequency) signal components.

6.3.1.5 Testing the resolution performance of TFDs for a signal with components of *different amplitudes*

We have shown that the spectrogram and the MBD are, based on the resolution performance measure P_i, two best-performing TFDs for representing the signal $s_4(t)$ consisting of three sinusoids. We now assess how the performance of these TFDs varies when the components' amplitudes of a two-sinusoid signal $s_5(t)$: (a) are equal, and (b) the second component amplitude is half of the first component amplitude (in time); both cases are studied for the following three separations between the two sinusoids: $\Delta f = 0.2$ Hz, $\Delta f = 0.1$ Hz, and $\Delta f = 0.05$ Hz.

TFD	$P_{i_1}(64)$	$P_{i_2}(64)$
Born–Jordan	0.8887	0.9029
Choi–Williams	0.9387	0.9580
Modified B	0.9566	0.9675
Spectrogram	0.9520	0.9631
Zhao–Atlas–Marks	0.8054	0.8128

TABLE 6.6. Instantaneous ($t = 64$) resolution performance assessment measure for TFDs of a three-component signal $s_4(t)$ for the pair of closer ($P_{i_1}(64)$) and the pair of more separated ($P_{i_2}(64)$) signal components.

Window	$\Delta f = f_2 - f_1$	A_2/A_1	$L = 127$	$L = 95$	$L = 63$	$L = 31$
Rectangular	0.2	1	0.8623	0.8782	0.8797	0.8686
		1/2	0.8235	0.8533	0.8458	0.8253
	0.1	1	0.8952	0.8643	0.8741	0.8281
		1/2	0.8746	0.8328	0.8324	0.8097
	0.05	1	0.8279	0.8369	0.8663	0.8010
		1/2	0.7941	0.8010	0.8087	0.5116
Hamming	0.2	1	0.9682	0.9646	0.9570	0.9316
		1/2	0.9644	0.9589	0.9519	0.9282
	0.1	1	0.9576	0.9545	0.9381	0.9151
		1/2	0.9534	0.9495	0.9334	0.9129
	0.05	1	0.9403	0.9163	0.8682	0
		1/2	0.9351	0.9175	0.8782	0.8704

TABLE 6.7. Assessment of the resolution performance (at $t = 64$) for the spectrogram of a two-sinusoid signal $s_5(t)$ for different ratios of the components' mainlobe amplitudes A_2/A_1 and different components' frequency separations Δf. The spectrogram is calculated using the rectangular and Hamming windows of length L.

Table 6.7 summarizes the performance results (at the time instant $t = 64$) obtained for the signal spectrogram with the rectangular and Hamming windows (of four different lengths). We observe that the resolution performance of the spectrogram with the Hamming window continuously decreases as the window length decreases from $L = 127$ to $L = 31$ for both equal and nonequal amplitudes of the components for *all* three frequency separations between these components. The difference in the P_i values becomes larger as the components get closer in frequency, and so their resolution becomes more critical. The spectrogram with the rectangular window does not show this trend of the continuous decrease in its resolution performance, since, unlike the Hamming window case, its optimal window length ($L_{opt} = 107$) is smaller than the signal duration $T = 128$.

Table 6.8 gives the performance results (at the time instant $t = 64$) for the MBD of signal $s_5(t)$ for a range of its kernel filter parameter values. It indicates that for both the equal and nonequal amplitude components the resolution performance of the MBD continuously decreases as the parameter β increases, regardless of the components' frequency separation. This is due to the fact that, for large β, cross-terms are less attenuated by the more-spread kernel filter in the ambiguity domain, and the large values of the cross-term amplitude A_X in the (t, f) domain reduce the resolution performance measure P_i.

This test illustrates that the measure P_i provides a good assessment of TFDs' resolution performance for signals with different components' amplitudes and different time-varying components' frequency separations.

$\Delta f = f_2 - f_1$	A_2/A_1	$\beta = 10^{-4}$	$\beta = 10^{-3}$	$\beta = 10^{-2}$	$\beta = 10^{-1}$
0.2	1	0.9700	0.9211	0.8757	0.8683
	1/2	0.9664	0.9054	0.8365	0.8263
0.1	1	0.9611	0.9236	0.8933	0.8813
	1/2	0.9568	0.9065	0.8622	0.8590
0.05	1	0.9436	0.8938	0.8520	0.7011
	1/2	0.9412	0.8822	0.8199	0.4610

TABLE 6.8. Assessment of the resolution performance (at $t = 64$) for the MBD (for four values of its kernel filter parameter β) of a two-sinusoid signal $s_5(t)$ for different ratios of the components' mainlobe amplitudes A_2/A_1 and different components' frequency separations Δf.

6.3.2 *Selecting the optimal TFD for real-life signals under given constraints*

As mentioned earlier, different TFDs display information in the time-frequency plane with a varying amount of detail and "accuracy." In an application, selecting a TFD that does this in the optimal way is a critical factor when applying time-frequency analysis to real-life signals.

Based on the concept of multiple view TFDs [26], we define in this subsection the methodology for the selection of the optimal TFD, under application-specific constraints, for real-life signals in time-frequency regions where signal features of interest are located.

6.3.2.1 Methodology

The methodology consists of the following steps.

1. Represent the signal in the (t, f) domain using the WVD, the spectrogram, and the MBD. These three TFDs will provide us with indications of the main signal features in the time-frequency plane: the number of components, their relative amplitudes, the components' durations and bandwidths (features obtained from the MBD and the spectrogram), as well as the cross-terms locations (obtained from the signal WVD).
   The WVD is essentially a parameter-free TFD, while the key parameters of the spectrogram and MBD (the window type and length, and the kernel filter parameter β, respectively) need to be initialized. For the spectrogram, we use the Hanning window as the initial window type, and from several window lengths (short, medium, and long—whose values depend on the signal time duration) select as the initial window length the one that results in the "cleanest" time-frequency plot. This window length is also used as the initial effective window length [3] for all other TFDs considered in the application. In the case of MBD, the initial value for β is set to 0.001. The choice of these initial parameter values

is based on the fact that the spectrogram with the Hanning window and MBD with $\beta \leq 0.001$ have been found to perform well for the majority of signals whose TFDs' resolution performance we have analyzed in [1,2,27,28].

2. Using these three TFDs, identify regions in the (t, f) domain where application-specific signal features (e.g., closely-spaced components, crossing components, sudden changes in component IF laws) are located. We call such regions the regions of interest (ROIs). The ROIs are rectangles in the time-frequency plane whose dimensions are the "time of interest" and the "frequency of interest." The time (resp. frequency) of interest is the time interval (resp. frequency band) of the TFD where the specific signal features are located in time (resp. frequency).
3. For each selected ROI, optimize different TFDs under application-given constraints.
4. Select as the signal optimal TFD, the TFD which among other considered optimised TFDs best satisfies *each* of the given constraints in *all* observed ROIs.

6.3.2.2 Optimal TFD selection for the unbiased, efficient, multicomponent IF estimation of the Noisy Minor song signal

In this section we illustrate the use of our methodology for the "Noisy Minor" (*Manorina melanocephala*) Australian bird song signal [18]. The constraint that needs to be satisfied is the unbiased, efficient, multicomponent IF estimation in (t, f) regions where the signal components are closely-spaced.

Figure 6.20(a) shows the signal time-domain plot, which indicates how its amplitude varies with time, and Figure 6.20(b) (the signal PSD) shows which frequencies (with which magnitudes) are present in the signal. However, neither of the two can provide us with information on the signal internal structure (the number of signal

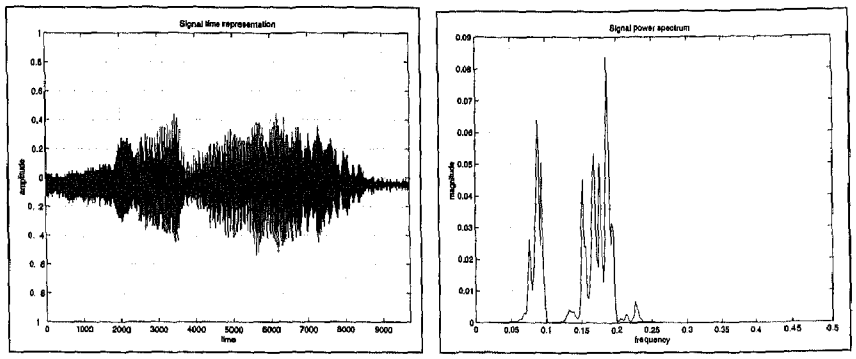

(a) Time-domain (b) Frequency-domain

FIGURE 6.20. Time-domain and frequency-domain representations of the Noisy Minor song signal.

components, their relative amplitudes, IF laws, time intervals and frequency bands these components occupy, etc.).

To have a more complete "picture" of this signal, we analyze it in the (t, f) domain. This requires identifying a TFD that is optimal for the signal. By employing the steps of the above-defined methodology, we find in this example the regionally optimal TFD of the Noisy Minor song signal for efficient and unbiased estimations of the signal components' IFs from the TFD's peaks [2, 3, 6] in the (t, f) regions where these components form closely spaced pairs.

We start by representing the signal in the (t, f) plane using the WVD, MBD ($\beta = 0.001$), and the spectrogram with Hanning window of length 511. In selecting the optimal window length for the spectrogram, other lengths (127, 255, 1023) were also tested, but length 511 resulted in the most clear (t, f) plot of the signal spectrogram. The effective window length for the WVD and the MBD is also initially set to 511. By comparing the plots of these TFDs, several components (dominant ridges) are identified in the signal, and four ROI are defined where these components are closely spaced to each other in the time-frequency plane (see Figure 6.21).

In order to meet the accurate IFs estimation constraint, we first need to optimize the resolution performance of TFDs in the selected ROIs by applying the procedure defined in Subsection 6.3.1.1. Table 6.9 lists the TFDs' resolution optimization results. It shows that the MBD with $\beta = 5 \times 10^{-5}$, having the largest optimal performance measure P_{opt} (the regional performance measure corresponding to the optimal value of the TFD kernel filter parameter) among the eight considered TFDs, achieves the best resolution of the signal components in ROI_1. It slightly outperforms the smoothed WVD (with the Hamming window of length 415 chosen as

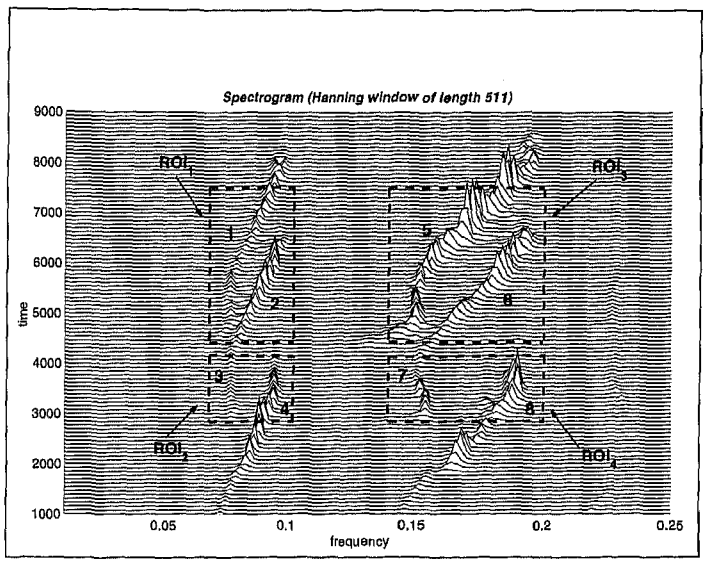

FIGURE 6.21. ROIs for the Noisy Minor song signal's time-frequency distributions.

the smoothing window) and the spectrogram (with the Hanning window of length 447). Other TFDs, even after being optimized in ROI_1, still do not achieve as good resolution performance as the MBD does. The Rihaczek distribution and WVD in particular perform poorly, as indicated by their P_{opt} values of 0.5825 and 0.4984, respectively.

Figure 6.8 shows the ROI_1 of the optimized TFDs of the Noisy Minor song signal. Note that P_{opt} ranks the TFDs in accordance with our visual impressions of their (t, f) plots; i.e., the clearer the plot is (good components' concentration and less interference present in the TFD), the larger P_{opt} is obtained.

Similar analyses can be done for ROI_2, ROI_3 and ROI_4. What is interesting to observe is that the spectrogram has the best resolution performance in each of ROI_2, ROI_3, and ROI_4. The spectrogram's performance closely approaches that of the MBD in ROI_1 too. The three best-performing TFDs for all ROIs considered in this example, with very similar resolution performances, are the MBD, the smoothed WVD, and the spectrogram. The fact that more than one TFD perform well for a certain signal can be of benefit to the signal analyst, giving him/her more freedom in selecting the signal optimal TFD under application-specific constraints.

Having dealt with the requirement for a good (t, f) resolution of closely spaced components of the Noisy Minor song signal, we now select the signal TFD that allows for the most accurate components' IFs estimation (from the peaks of the TFD's dominant ridges) in each of the observed ROIs. Among the three best-performing TFDs, only the MBD provides unbiased and efficient multicomponent FM signals' IF estimates [5]. Therefore, under the given accurate multicomponent IF estimation constraint, we select the Modified B distribution as the *optimal TFD* of the Noisy Minor song signal, *for all four ROIs*. The optimal value of the MBD kernel filter parameter β slightly varies across the ROIs, so that in each of these regions the best resolution of the signal components is achieved; as required by the robust multicomponent IF estimation techniques [2].

6.4 Discussion and conclusions

This chapter brings together, in a heuristic way, three key recent developments that are fundamental to a better understanding and use of time-frequency signal analysis tools.

The first development consists of a concise, updated presentation of the core concepts of TFSP, including a simple way of designing high resolution TFDs for real-life practical applications.

The second development consists of using a quantitative measure of goodness for TFDs to compare the resolution performance of time-frequency distributions for multicomponent signals analysis. This result fills an obvious need for the practitioner in that, until recently, the comparison of the resolution performance of TFDs was primarily based on a visual impression of the TFDs' plots. The introduction of the resolution performance measure for quadratic TFDs has led to an improvement in the design of tools for high resolution time-frequency analysis of multicomponent

TFD	ROI_1		ROI_2		ROI_3		ROI_4	
	P_{opt}	*Parameter*	P_{opt}	*Parameter*	P_{opt}	*Parameter*	P_{opt}	*Parameter*
Born–Jordan	0.7574	N/A	0.9005	N/A	0.8647	N/A	0.8837	N/A
Choi–Williams	0.8755	3	0.9323	0.09	0.8723	0.3	0.9077	3
Modified B	0.9198	5×10^{-5}	0.9433	6×10^{-5}	0.8907	4×10^{-4}	0.9602	3×10^{-5}
Rihaczek	0.5825	N/A	0.7883	N/A	0.6260	N/A	0.6916	N/A
Smoothed Wigner–Ville	0.9195	Hamm, 415	0.9420	Bart, 383	0.8879	Bart, 159	0.9534	Rect, 287
Spectrogram	0.9145	Hann, 447	0.9574	Bart, 383	0.9261	Hann, 223	0.9710	Bart, 447
Wigner–Ville	0.4984	N/A	0.7858	N/A	0.6077	N/A	0.5813	N/A
Zhao–Atlas–Marks	0.7900	1	0.8409	1	0.7922	3	0.8191	2

TABLE 6.9. The optimal resolution performance measures P_{opt} and the corresponding optimal kernel filter parameter values of TFDs of the Noisy Minor song signal for the four time-frequency ROIs defined in Figure 6.21.

signals, by removing unnecessary limitations in the way desirable properties of TFDs were previously chosen. The MBD, which outperforms existing TFDs in terms of (t, f) resolution for signals with closely spaced components, was introduced in this way.

Thirdly, a methodology for selecting an optimal TFD for a given real-life signal under application-specific constraints has been defined. The use of the methodology in practice was illustrated on an Australian bird song signal, for which the optimal TFD for an accurate multicomponent IF estimation was found in several time-frequency ROI.

The results presented in this chapter are important for the field of TFSP. They not only allow for the optimal selection of a specific application-dependent TFD, but also open the way for further research in developing high resolution digital signal processing tools for nonstationary signals, by providing a measure of quality of TFDs and removing often unnecessary TFD design limitations.

References

[1] B. Boashash and V. Sucic, A resolution performance measure for quadratic time-frequency distributions. In *Proc. 10th IEEE Workshop on Statistical Signal and Array Processing, SSAP 2000*, pages 584–588, Pocono Manor, PA, USA, August 2000.

[2] B. Boashash, editor, *Time-Frequency Signal Analysis and Processing*. Prentice-Hall, Englewood Cliffs, NJ, 2003.

[3] B. Boashash, Time–frequency signal analysis. In S. Haykin, editor, *Advances in Spectrum Analysis and Array Processing*, volume 1, chapter 9, pages 418–517. Prentice-Hall, Englewood Cliffs, NJ, 1991.

[4] B. Boashash, Estimating and interpreting the instantaneous frequency of a signal—part 1: Fundamentals, part 2: Algorithms and applications. *Proceedings of the IEEE*, 80(4):519–568, April 1992.

[5] Z. M. Hussain and B. Boashash, Multi-component IF estimation. In *Proc.* 10^{th} *IEEE Workshop on Statistical Signal and Array Processing, SSAP 2000*, pages 559–563, Pocono Manor, PA, USA, August 2000.

[6] B. Boashash, editor, *Time-Frequency Signal Analysis. Methods and Applications*. Longman–Cheshire/Wiley, Melbourne/New York, 1992.

[7] L. Cohen, *Time-Frequency Analysis*. Prentice-Hall, Englewood Cliffs, NJ, 1995.

[8] C. H. Page, Instantaneous power spectra. *Journal of Applied Physics*, 23(1):103–106, January 1952.

[9] D. Gabor, Theory of communication. *Journal of IEE*, 93:429–457, 1946.

[10] L. Cohen, Time-frequency distributions—a review. *Proceedings of the IEEE*, 77(7):941–981, July 1989.

[11] P. Z. Peebles, *Probability, Random Variables and Random Signal Principles*. McGraw-Hill, New York, NY, 4th edition, 2001.

[12] P. Flandrin, Some features of time-frequency representation of multicomponent signals. In *Proc. IEEE Int. Conf. on Acoustics, Speech and Signal Processing, ICASSP 1984*, pages 41.B.4.1–4, San Diego, CA, USA, March 1984.

3] H. Choi and W. Williams, Improved time-frequency representation of multicomponent signals using exponential kernels. *IEEE Transactions on Acoustics, Speech and Signal Processing*, 37(6):862–871, June 1989.

4] B. Barkat and B. Boashash, A high–resolution quadratic time–frequency distribution for multicomponent signals analysis. *IEEE Transactions on Signal Processing*, 49(10):2232–2239, October 2001.

5] Lj. Stankovic, An analysis of some time-frequency and time-scale distributions. *Annales–des–Telecommunications*, 49(9–10):505–517, September/October 1994.

6] Lj. Stankovic, Auto-term representation by the reduced interference distributions: A procedure for kernel design. *IEEE Transactions on Signal Processing*, 44(6):1557–1563, June 1996.

7] M. G. Amin and W. Williams, High spectral resolution time-frequency distribution kernels. *IEEE Transactions on Signal Processing*, 46(10):2796–2803, October 1998.

8] John Gould's Birds of Australia, RMB 4375, Seymour 3660, Victoria, Australia, On CD-ROM.

9] Y. Zhao, R. J. Marks, and L. E. Atlas, The use of cone-shaped kernels for generalised time-frequency representations of nonstationary signals. *IEEE Transactions on Acoustics, Speech and Signal Processing*, 38(7):1082–1091, July 1990.

10] D. Jones and T. Parks, A high resolution data-adaptive time-frequency representation. *IEEE Transactions on Acoustics, Speech and Signal Processing*, 38(12):2127–2135, December 1990.

11] W. J. Williams and T. Sang, Adaptive RID kernels which minimize time-frequency uncertainty. In *Proc. IEEE–SP Int. Symposium on Time-Frequency and Time-Scale Analysis*, pages 96–99, Philadelphia, PA, USA, October 1994.

12] T. H. Sang and W. J. Williams, Renyi information and signal-dependent optimal kernel design. In *Proc. IEEE Int. Conf. on Acoustics, Speech and Signal Processing, ICASSP 1995*, volume 2, pages 997–1000, Detroit, MI, USA, May 1995.

13] P. Oliviera and V. Barosso, Uncertainty in the time-frequency plane. In *Proc. 10th IEEE Workshop on Statistical Signal and Array Processing, SSAP 2000*, pages 607–611, Pocono Manor, PA, USA, August 2000.

14] V. Sucic and B. Boashash, On the selection of quadratic time-frequency distributions and optimisation of their parameters. In *Proc. 3rd Australasian Workshop on Signal Processing Applications, WoSPA 2000*, Brisbane, Australia, December 2000. On CD-ROM.

15] V. Sucic, B. Barkat, and B. Boashash, Performance evaluation of the B-distribution. In *Proc. 5th Int. Symposium on Signal Processing and Its Applications, ISSPA 1999*, volume 1, pages 267–270, Brisbane, Australia, August 1999.

16] G. Frazer and B. Boashash, Multiple view time-frequency distributions. In *Proc. 27th Asilomar Conference on Signals, Systems and Computers*, volume 1, pages 513–517, Los Alamitos, CA, USA, 1993.

17] V. Sucic and B. Boashash, Parameter selection for optimising time-frequency distributions and measurements of time-frequency characteristics of non-stationary signals. In *Proc. IEEE Int. Conf. on Acoustics, Speech and Signal Processing, ICASSP 2001*, volume 6, pages 3557–3560, Salt Lake City, UT, USA, May 2001.

18] V. Sucic and B. Boashash, Optimisation algorithm for selecting quadratic time-frequency distributions: Performance results and calibration. In *Proc. 6th Int. Symposium on Signal Processing and Its Applications, ISSPA 2001*, volume 1, pages 331–334, Kuala-Lumpur, Malaysia, August 2001.